

THE SIMULTANEOUS RETRIEVAL EXPORT PACKAGE

W. L. Smith¹, H. M. Woolf², C. M. Hayden², A. J. Schreiner¹
Cooperative Institute for Meteorological Satellite Studies
University of Wisconsin
Madison, Wisconsin 53706, USA

¹ Space Science and Engineering Center

² NOAA/NESDIS

1. INTRODUCTION

As part of the "First International TOVS Study Conference", a description of a physical algorithm for retrieving temperature and moisture soundings from TOVS radiance data was described (Smith et al., 1983). This algorithm was incorporated into the "TOVS Export Package" made available by CIMSS to direct readout users of TOVS data. The physical algorithm consisted of the application of the Smith-Iterative Solution (Smith, 1970) for temperature and moisture profiles. In that approach, (1) an initial profile for temperature and water vapor is specified from climatology, statistical regression, or from an NWP model, (2) radiances are calculated from the initial profiles, (3) the temperature profile is adjusted in an iterative manner until there is agreement between the observed and calculated radiances in the cloud insensitive microwave O_2 channels, (4) the infrared window channels are used to define either the surface skin temperature or the temperature of cloud within the instrument's field of view and the cloud level is defined using the microwave specified temperature profile, (5) the guess moisture profile is adjusted to reflect the existence of cloud by assuming 100% relative humidity at the cloud level and then further adjusted in an iterative manner in order to achieve convergence between observed and calculated radiance for the water vapor channels, and (6) the temperature profile is then further adjusted in an iterative manner in order to achieve convergence between the radiances observed and calculated in the infrared CO_2 channels.

Since the first Igl's conference, a new retrieval algorithm has been developed which permits the simultaneous retrieval of surface-skin (or cloud) temperature, and the temperature and moisture profiles. The advantage of the "simultaneous solution" is two-fold: (1) the radiances observed in all channels are used to solve for all parameters simultaneously, thus alleviating the problem of the interdependence of the radiance observation upon the three parameters, and (2) since a direct analytical solution is employed, the process is computationally efficient.

In this paper the new algorithm now incorporated in the "TOVS export package" is described. As with the prior "iterative" algorithm, the physical nature of the solution permits the influence of surface variables (i.e., terrain elevation, emissivity, and temperature) and cloudiness to be accounted for in the profile determinations. The cloud handling algorithm

is modified to enable the infrared data to be utilized in partly cloudy as well as cloud overcast sky conditions. The low sensitivity of the simultaneous solution to the initial guess profile and the improved performance of the simultaneous retrieval method compared to the previously established iterative technique (Smith et al., 1983; Susskind, 1984) are demonstrated from TOVS orbits over Europe obtained during the ALPine EXperiment (ALPEX) as selected by the International Radiation Commission's TOVS Working Group for the intercomparison of retrieval methods. The physics for treating surface emissivity, terrain elevation, and reflected sunlight are not described here since these aspects have been provided in the previous report (Smith et al., 1983).

2. DIRECT PHYSICAL SOLUTION

An important advance in the profile retrieval methodology is the simultaneous temperature and water vapor solution (Smith and Woolf, 1984). In order to achieve the simultaneous solution, the integral form of the radiative transfer equation is integrated by parts and treated in the perturbation form:

$$\delta T^* = \int_0^P \delta U \frac{\partial T}{\partial p} \frac{\partial \tau}{\partial U} \frac{(\partial B / \partial T)}{(\partial B / \partial T^*)} dp - \int_0^P \delta T \frac{\partial \tau}{\partial p} \frac{(\partial B / \partial T)}{(\partial B / \partial T^*)} dp + \delta T_s \frac{(\partial B_s / \partial T_s)}{(\partial B / \partial T^*)} \quad (1)$$

where T^* is brightness temperature, U is precipitable water vapor, B is Planck radiance, T is temperature, T_s is surface-skin temperature, τ is transmittance, and p is pressure. The perturbation, δ , is with respect to an a-priori estimated or mean condition. The pressure dependence of all integrand variables is to be understood. In order to solve (1) for δU , δT , and δT_s from a set of spectrally independent radiance observations, the perturbation profiles are represented in terms of arbitrary pressure functions, $\phi(p)$:

$$\delta q(p) = g \sum_{i=1}^N \alpha_i q_0(p) \phi_i(p) \quad (2a)$$

$$\delta T(p) = - \sum_{i=N+1}^N \alpha_i \phi_i(p) \quad (2b)$$

where $q(p)$ is the water vapor mixing ratio and g is gravity. The zero subscript indicates the a priori condition. Equation 2a implies from the gas law and hydrostatic equation that

$$\delta U(p) = \sum_{i=1}^N \alpha_i \int_0^P q_0(p) \phi_i(p) dp \quad (2c)$$

Substituting representations (2b) and (2c) into (1) and letting $\alpha_0 = \delta T_s$ yields for each spectral radiance observation, δT_j^* , for a set of K spectral channels:

$$\delta T_j^* = \sum_{i=0}^M \alpha_i \phi_{ij} \quad j=1,2,\dots,K \quad (3)$$

where

$$\phi_{0,j} = \frac{\partial B_j / \partial T_s}{\partial B_j / \partial T_j^*} \tau_{s,j}$$

$$\phi_{i,j} = \int_0^P \int_0^P [q_0 \phi_i dp] \left[\frac{\partial T}{\partial p} \frac{\partial \tau_j}{\partial U} \frac{\partial B_j / \partial T}{\partial B_j / \partial T_j^*} \right] dp \quad i \leq N \quad (4)$$

$$\phi_{i,j} = \int_0^{P_s} \phi_i \left[\frac{\partial \tau_j}{\partial p} \frac{\partial B_j / \partial T}{\partial B_j / \partial T_j^*} \right] dp \quad N < i \leq M.$$

The $\phi_{i,j}$ quantities are calculated from the a-priori estimated or mean profile conditions. Written in matrix form

$$t^* = \phi \alpha \quad (5)$$

where t^* is a row vector of K radiance observations, α is a row vector of $M+1$ coefficients, and ϕ is a matrix having dimensions $(K \times M+1)$. Assuming that $K \geq M+1$, then the least squares solution of (5) is employed to give

$$\alpha = (\phi^T \phi)^{-1} \phi^T t^* \sim (\phi^T \phi + \gamma I)^{-1} \phi^T t^* \quad (6)$$

where $()^T$ indicates matrix transposition and $()^{-1}$ indicates matrix inverse. The γI term, where γ (nominally 0.1) is a scalar and I is the identity matrix, is incorporated to stabilize the matrix inverse. Once the α_i 's are determined, δT_s , δq , and δT are specified from (2) and added to the a-priori estimates to yield the final solutions for surface-skin temperature and the water vapor mixing ratio and temperature profiles.

The choice of pressure basis functions $\phi(p)$ is arbitrary. For example, empirical orthogonal functions (i.e., eigenvectors of the water vapor and temperature profile covariance matrices) can be used in order to include statistical information in the solution. However, here for its application to the TIROS Operational Vertical Sounder (TOVS) data, physical functions, the profile weighting functions ($d\tau/d\ln p$) of the radiative transfer equation, are used as the basis functions.

Ancillary information such as surface observations can be easily incorporated into the profile solutions. For example, for surface observations it follows from (2) that

$$q(p_s) - q_o(p_s) = g \sum_{i=1}^N \alpha_i q_o(p_s) \phi_i(p_s) \quad (7)$$

and

$$T(p_s) - T_o(p_s) = - \sum_{i=N+1}^M \alpha_i \phi_i(p_s) \quad (8)$$

have the same form as (3) and therefore can be added to the set to yield K+2 equations to solve for M+1 unknowns (α).

The main advantage of the "simultaneous" retrieval method is that it enables the temperature and water vapor profiles and the surface skin temperature to be determined simultaneously using all the radiance information available. The simultaneity directly addresses the problems associated with water vapor radiance dependence upon temperature and the dependence of several of the carbon dioxide channel radiance observations used for temperature profiling, on the water vapor concentration. The dependence of the radiance observations on surface emissions is accounted for in the simultaneous solution by the inclusion of surface temperature as an unknown. Also, since only a single matrix inversion is required for the specification of all parameters, the solution is more computationally efficient than the iterative technique. Finally, but significantly, ancillary observations of temperature and/or moisture from surface sensors or aircraft, for example, can be readily incorporated in the solution.

Logistics

The processing of the TOVS data begins with the specification of an initial profile including surface observations, if available. The initial profile can be specified either from climatology or through the use of regression coefficients, based either on synthetic radiances or on real radiances matched to radiosonde observations. The climatological and regression generated initial profile algorithms are internal to the Export Package. A third option exists whereby an analysis or forecast generated grid field of temperature and water vapor profiles can be used to create initial profiles. In this case the grid fields are external to the Export Package as are the surface data grid fields.

MSU and HIRS radiances are obtained for a 3 x 3 array (75 km resolution) of HIRS FOV's, as described in the earlier report (Smith et al., 1983); the MSU data having been interpolated to each HIRS FOV. These are used in a two step procedure to generate an initial solution, to estimate cloud contamination, and to produce final estimates of temperature and moisture as follows:

Step 1: The stratospheric HIRS brightness temperatures (channels 1-3), the MSU brightness temperatures (MSU 1-4), and the middle and upper tropospheric HIRS water vapor channels (HIRS 11 and 12) are used to derive a first estimate of the temperature and moisture profile for the sounding location. With this channel selection, the estimate should be relatively free of error due to cloud attenuation. The weighting functions for HIRS-1 and MSU 2-4 are utilized as the basis functions for temperature and the HIRS

7 and 12 weighting functions are used as the basis functions for water vapor in the initial retrieval. Once the first estimate of the temperature and water vapor profile is achieved, the height and amount of any cloud affecting the infrared observations are determined by the method described in the next section. After this is accomplished all channels (except HIRS channels 13-19 in the cloudy case) are used to calculate the final surface temperature and the temperature and water vapor profiles.

Step 2: For the achievement of the final profile estimates the weighting functions for HIRS 1, 3, 7 and MSU 2-4 are used as the temperature profile basis functions, and those for HIRS 7, 11, and 12 are used as the water vapor profile basis functions. Since as many as nineteen different spectral radiance observations are used for the surface temperature and profile retrievals, the system of equations to be inverted is heavily overdetermined, thereby stabilizing the solution. (It should be noted that ozone and geopotential height are determined in the same manner as described for the iterative solution Export Package.)

Handling the Influence of Clouds

In the TOVS data processing, soundings are derived from a 3 x 3 matrix of HIRS fields of view (FOV), the Microwave Sounding Unit (MSU) data being spatially interpolated to the location of the HIRS spots. From the array, the observations for the "clearest" FOV's, defined as those whose 11 μ m radiance values are within 2°K of the local maximum, are averaged for the sounding determination. The magnitude of the visible channel reflectance and the 3.7 μ m, 4.0 μ m, and 11 μ m window channel brightness temperatures are used in conjunction with surface temperature observations, if available, to specify whether the "clearest" radiances are contaminated by clouds. If the radiances are determined to be affected by clouds, their pressure height and fractional coverage are specified on the basis of certain CO₂ channel infrared radiances and the microwave radiance specified temperature profile. The cloud height is calculated using the CO₂ slicing technique (Smith and Platt, 1977, Menzel et al., 1983) from the relation

$$\frac{I(\nu_1) - \hat{I}_c(\nu_1)}{I(\nu_2) - \hat{I}_c(\nu_2)} = \frac{\int_{P_c}^{P_o} \tau(\nu_1, p) \frac{\partial B(\nu_1, \hat{T})}{\partial p} dp}{\int_{P_c}^{P_o} \tau(\nu_2, p) \frac{\partial B(\nu_2, \hat{T})}{\partial p} dp} \quad (9)$$

where $\hat{I}_c(2)$ is the clear-column radiance calculated from the microwave specified temperature profile, T , and ν_1 and ν_2 refer to HIRS channels 5 and 7 respectively. The cloud pressure P_c is obtained by trial and error. The cloud fraction, N , is then obtained from the relation

$$N = \frac{I(\nu_1) - \hat{I}_c(\nu_1)}{I(\nu_2) - \hat{I}_c(\nu_2)} \quad (10)$$

where $\hat{I}_{cd}(v_1)$ is the radiance calculated for an opaque cloud overcast condition.

Given P_c and N , the guess mixing ratio profile is adjusted by assuming that the mixing ratio at the cloud level is given by

$$W(p_c) = N W_{sat} [\hat{T}(p_c)] + (1 - N) \hat{W}(p_c) \quad (11)$$

where W_{sat} is the saturation mixing ratio corresponding to the microwave specified temperature at the cloud pressure P_c and W is the original guess value of mixing ratio. Below the cloud a new guess mixing profile is achieved by interpolation using the original surface mixing ratio value.

Once the cloud parameters and the guess mixing ratio profile are established the brightness temperature discrepancies from the guess conditions, δT^* , can be calculated, including the effects of cloud within the field of view of the HIRS instrument. For the infrared channels the effects of cloud in the solution of (4) can be properly included by assuming that

$$\tau = (1 - N) \tau^{orig} \quad (12)$$

for pressures greater than the cloud pressure. This transmittance function modification reduces the influence of the infrared observations on the solution below the cloud in proportion to the cloud obscuration. After this adjustment, the simultaneous solution proceeds exactly as in the clear sky condition.

3. RESULTS

Retrieval Analyses

In this section, objective analyses of the TOVS retrievals achieved using two independent initial guess profile procedures: (a) statistical regression using MSU brightness temperatures as predictors; and (b) climatology based on the U.S. Standard Supplemental Atmospheres, are compared for the March 4, 5 ALPEX data sets. The first guess profile specification procedures have been described in the previous ITOVS-I conference report. The analyses of the 75 Km resolution TOVS soundings were produced using the BARNES method (Barnes, 1973). These analyses are compared to each other and to the operational analyses of radiosonde data for this area by the European Center for Medium Range Weather Forecasting (ECMWF).

Figures 1-4 show the temperature analysis comparisons for the mandatory pressure levels from 850 mb to 300 mb, respectively. There is little difference between the analyses achieved from the two different first guess-based TOVS retrievals, indicating weak dependence of the simultaneous retrieval method on the first guess profile. Both sets of retrievals capture the rapid intensification of the trough over western Europe between 12 GMT of 4 March and 00 GMT of 5 March, 1982. The magnitude of the differences from the ECMWF analyses are generally less than 3°C. Curiously, the differences appear to be slightly smaller for the climatological first guess retrievals, particularly at the 300 mb level. It is also noteworthy that

the largest differences of the TOVS analyses from those of the ECMWF are generally over radiosonde data-void areas (e.g., the eastern North Atlantic and the Mediterranean). The largest differences between the two TOVS analyses are about 3°C at the 300 mb level over southeastern Europe.

Figure 5-8 show analyses of the TOVS dewpoint temperatures for the mandatory levels from 850 to 300 mb levels, respectively. Superimposed are the radiosonde values shown for verification. As with the temperature analyses, the analyses of the dewpoint temperatures reveal very close agreement between the "regression" and "climatology" first guess based retrievals. There is also very good qualitative agreement between the volume-sampled satellite dewpoints and the point sampled radiosonde observations. Most striking is the qualitative agreement between the highly structured 500 mb dewpoint temperatures and the radiosonde observations (Fig. 7). It is interesting to note that the gradients in the TOVS retrievals are as large, if not larger, than the values displayed by the radiosondes. Also, the radiosonde data appear somewhat "noisy" relative to the coherent analyses of the TOVS retrievals. Because of the gaps in the radiosonde, particularly over the Mediterranean region, it would be impossible to achieve analyses with the same degree of horizontal and temporal consistency as displayed in the TOVS analyses. The horizontal sampling limitation of the radiosonde data is even more striking at the 300 mb level where many of the latter are missing due to "motorboating."

Finally, Figure 9 shows a comparison of 500 mb dewpoint analyses achieved using the prior iterative retrieval method ("Export II"). The significant improvement achieved with the simultaneous method is striking. Similar improvements are obtained at the other pressure levels (not shown). We have found, in general, that the largest improvements gained by the simultaneous retrieval system ("Export III") over those achieved by the iterative retrieval method ("Export II") are in the moisture results.

Statistics

Statistical comparisons between the TOVS retrievals and the ECMWF analyses are restricted here to the root mean square deviation (RMSD) after the mean difference has been removed. Curves of the mean difference are not given because they are generally less than 2°C and very similar for the "regression" and "climatology" cases, except for the 300 mb level where there exists a 2°C mean difference between the two retrieval types.

For all the TOVS statistics, the ECMWF analyses serve as a standard of "truth" although this is an approximation as shown in Figure 10 where the RMSD of radiosonde data and the ECMWF analyses is shown. It is noted that the RMSD values range between 1.2 and 3.0°C which puts bounds on the validity of the "truth." As shown in Figures 10-14, the RMSD values for the TOVS retrievals are not significantly larger than the RMSD values for the radiosonde. Since radiosonde data believed to have an accuracy better than 0.5°C, the explanation for their large RMSD values can be attributed to the synoptic scale smoothing displayed by the ECMWF analyses and the volume sampled TOVS soundings.

Figure 11 compares RMSD values achieved from the simultaneous retrieval algorithm "Export III" with those achieved with the prior iterative retrieval method "Export II." As may be seen, there is consistent improvement of the "Export III" soundings over those achieved with "Export II," being as large as 0.5°C at individual levels. In fact, the RMSD values shown for the simultaneous retrieval method are not significantly larger than the radiosonde RMSD values (compare Figs. 10 and 11).

Figure 12 shows a comparison between the RMSD values for "Export III" for the "regression" and "climatology" first guess conditions. The differences are insignificant, except in the upper troposphere where the regression statistics apparently aid in the initialization of the tropopause structure. Because of the limited vertical resolution of the TOVS radiance observations, the initial guess tropopause structure is reflected in the retrieval.

Figure 13 shows the impact that surface data has on the TOVS simultaneous retrievals. As expected, the influence is largely confined to the atmosphere below the 700 mb level. As may be seen, however, it is important to use surface analyses in the retrieval process; otherwise the expected error in the results will almost double near the earth's surface.

4. CONCLUSIONS

A new and improved retrieval algorithm has been developed and included in the "Export III" software system for TOVS temperature and moisture sounding retrieval. Small, but significant improvements are shown for temperature profiling with very large improvements demonstrated in the moisture sounding capabilities of the TOVS. As with the prior "Export" software packages, Export III is available to interested users who should contact the CIMSS of the University of Wisconsin.

5. REFERENCES

- Barnes, S. L., 1973: Mesoscale objective analysis using weighted time-series observations. NOAA Tech. Memo. ERL NESL-62, National Severe Storms Laboratory, 1313 Halley Circle, Norman, OK 73069, 60 pp.
- Greaves, J. R., H. E. Montgomery, L. W. Uccellini, and D. L. Endres, 1982: AVE/VAS Field Experiment NASA/GSFC Technical Report X-903-82-17, September 1982.
- Smith, W. L., 1983: The retrieval of atmospheric profiles from VAS geostationary radiance observations. J. Atmos. Sci., 40, 2025-2035.
- Smith, W. L., H. M. Woolf, C. M. Hayden, A. J. Schreiner, and J. M. Le Marshall, 1983: The physical retrieval TOVS export package. Presented at the First International TOVS Study Conference, Iglis, Austria, 29 August - 2 September 1983.

Smith, W. L., and H. M. Woolf, 1984: Improved vertical soundings from an amalgamation of polar and geostationary radiance observations. Preprint volume: Conference on Satellite Meteorology/Remote Sensing and Applications, June 25-29, 1984, Clearwater Beach, Florida. Published by American Meteorological Society, Boston, Massachusetts.

Susskind, J., J. Rosenfield, D. Reuter, and M. T. Chahine: Remote Sensing of Weather and Climate Parameters from HIRS 2/MSU on TIROS-N, Journal of Geophysical Research, Vol. 89, No. C6, June 20, 1984.

4/WLS18/02

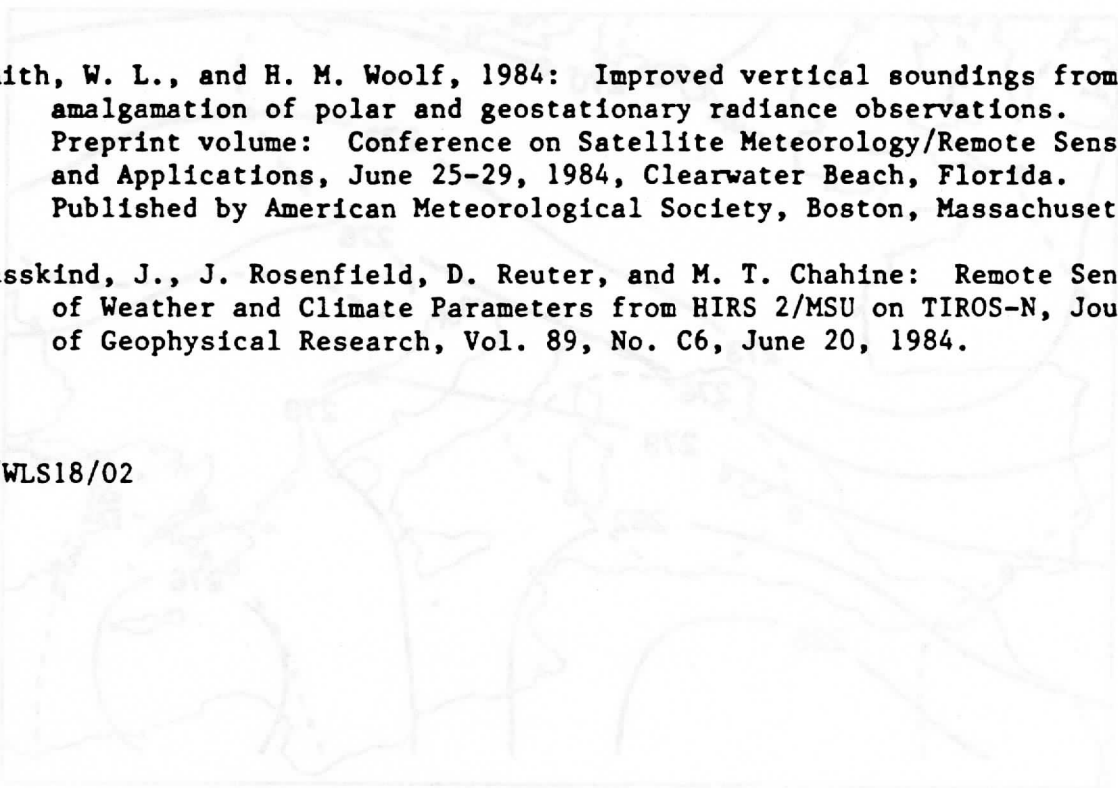
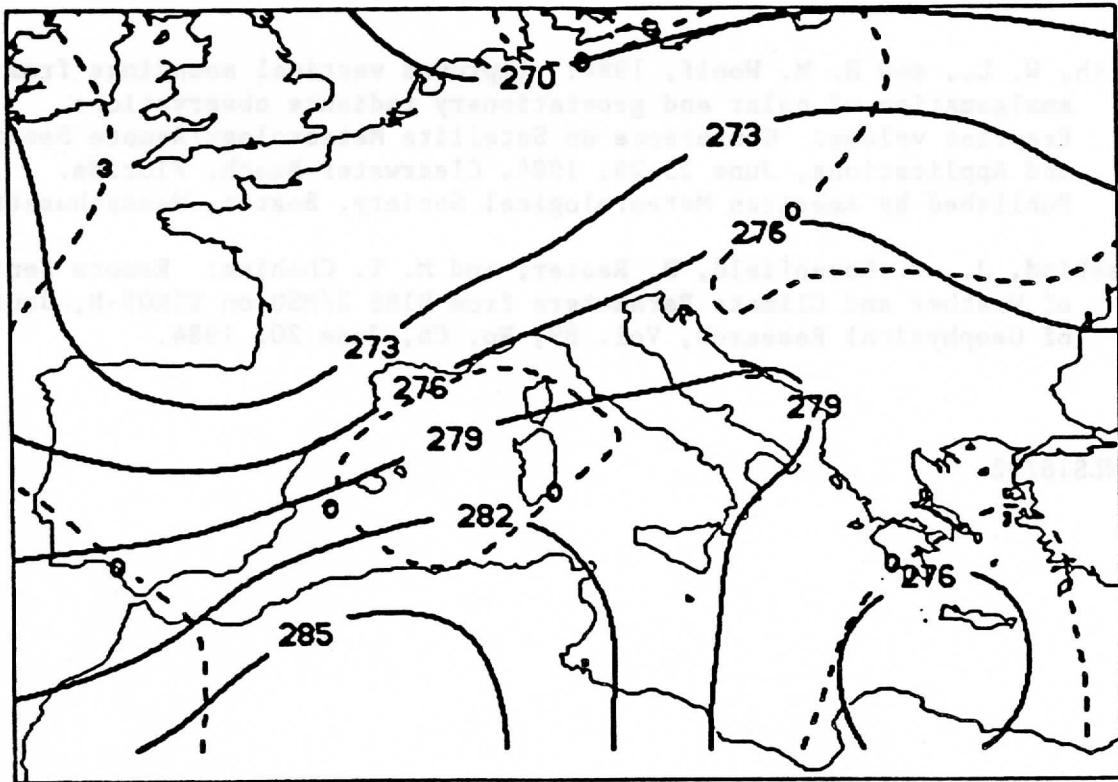


FIG. 1. Contour interval is 1 K. Contours are drawn at 1 K intervals. The contours are labeled with values such as 275, 270, 265, 260, 255, 250, 245, 240, 235, 230, 225, 220, 215, 210, 205, 200, 195, 190, 185, 180, 175, 170, 165, 160, 155, 150, 145, 140, 135, 130, 125, 120, 115, 110, 105, 100, 95, 90, 85, 80, 75, 70, 65, 60, 55, 50, 45, 40, 35, 30, 25, 20, 15, 10, 5, 0, -5, -10, -15, -20, -25, -30, -35, -40, -45, -50, -55, -60, -65, -70, -75, -80, -85, -90, -95, -100, -105, -110, -115, -120, -125, -130, -135, -140, -145, -150, -155, -160, -165, -170, -175, -180, -185, -190, -195, -200, -205, -210, -215, -220, -225, -230, -235, -240, -245, -250, -255, -260, -265, -270, -275, -280, -285, -290, -295, -300, -305, -310, -315, -320, -325, -330, -335, -340, -345, -350, -355, -360, -365, -370, -375, -380, -385, -390, -395, -400, -405, -410, -415, -420, -425, -430, -435, -440, -445, -450, -455, -460, -465, -470, -475, -480, -485, -490, -495, -500, -505, -510, -515, -520, -525, -530, -535, -540, -545, -550, -555, -560, -565, -570, -575, -580, -585, -590, -595, -600, -605, -610, -615, -620, -625, -630, -635, -640, -645, -650, -655, -660, -665, -670, -675, -680, -685, -690, -695, -700, -705, -710, -715, -720, -725, -730, -735, -740, -745, -750, -755, -760, -765, -770, -775, -780, -785, -790, -795, -800, -805, -810, -815, -820, -825, -830, -835, -840, -845, -850, -855, -860, -865, -870, -875, -880, -885, -890, -895, -900, -905, -910, -915, -920, -925, -930, -935, -940, -945, -950, -955, -960, -965, -970, -975, -980, -985, -990, -995, -1000.



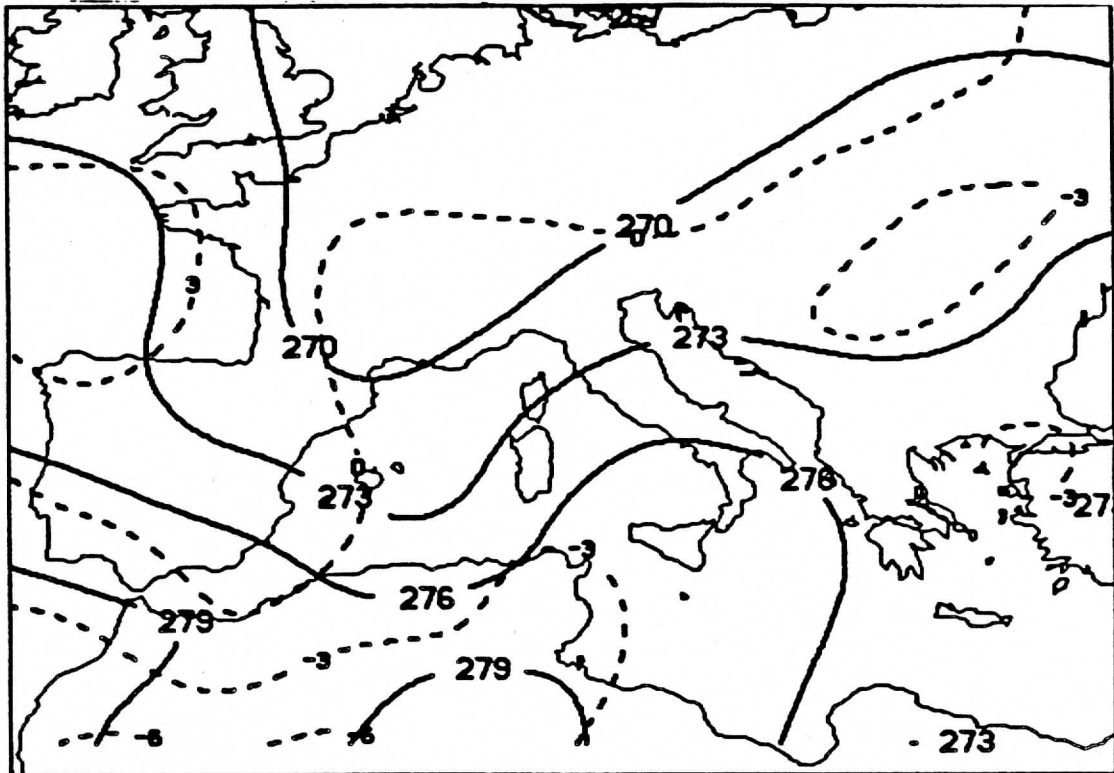
FIG. 2. Contour interval is 1 K. Contours are drawn at 1 K intervals. The contours are labeled with values such as 275, 270, 265, 260, 255, 250, 245, 240, 235, 230, 225, 220, 215, 210, 205, 200, 195, 190, 185, 180, 175, 170, 165, 160, 155, 150, 145, 140, 135, 130, 125, 120, 115, 110, 105, 100, 95, 90, 85, 80, 75, 70, 65, 60, 55, 50, 45, 40, 35, 30, 25, 20, 15, 10, 5, 0, -5, -10, -15, -20, -25, -30, -35, -40, -45, -50, -55, -60, -65, -70, -75, -80, -85, -90, -95, -100, -105, -110, -115, -120, -125, -130, -135, -140, -145, -150, -155, -160, -165, -170, -175, -180, -185, -190, -195, -200, -205, -210, -215, -220, -225, -230, -235, -240, -245, -250, -255, -260, -265, -270, -275, -280, -285, -290, -295, -300, -305, -310, -315, -320, -325, -330, -335, -340, -345, -350, -355, -360, -365, -370, -375, -380, -385, -390, -395, -400, -405, -410, -415, -420, -425, -430, -435, -440, -445, -450, -455, -460, -465, -470, -475, -480, -485, -490, -495, -500, -505, -510, -515, -520, -525, -530, -535, -540, -545, -550, -555, -560, -565, -570, -575, -580, -585, -590, -595, -600, -605, -610, -615, -620, -625, -630, -635, -640, -645, -650, -655, -660, -665, -670, -675, -680, -685, -690, -695, -700, -705, -710, -715, -720, -725, -730, -735, -740, -745, -750, -755, -760, -765, -770, -775, -780, -785, -790, -795, -800, -805, -810, -815, -820, -825, -830, -835, -840, -845, -850, -855, -860, -865, -870, -875, -880, -885, -890, -895, -900, -905, -910, -915, -920, -925, -930, -935, -940, -945, -950, -955, -960, -965, -970, -975, -980, -985, -990, -995, -1000.



4 MARCH 1982 1200GMT
850MB T(K)

REGRESSION
SAT ANAL(SOLID) ECMWF - SAT ANAL(DASHED)

(a)

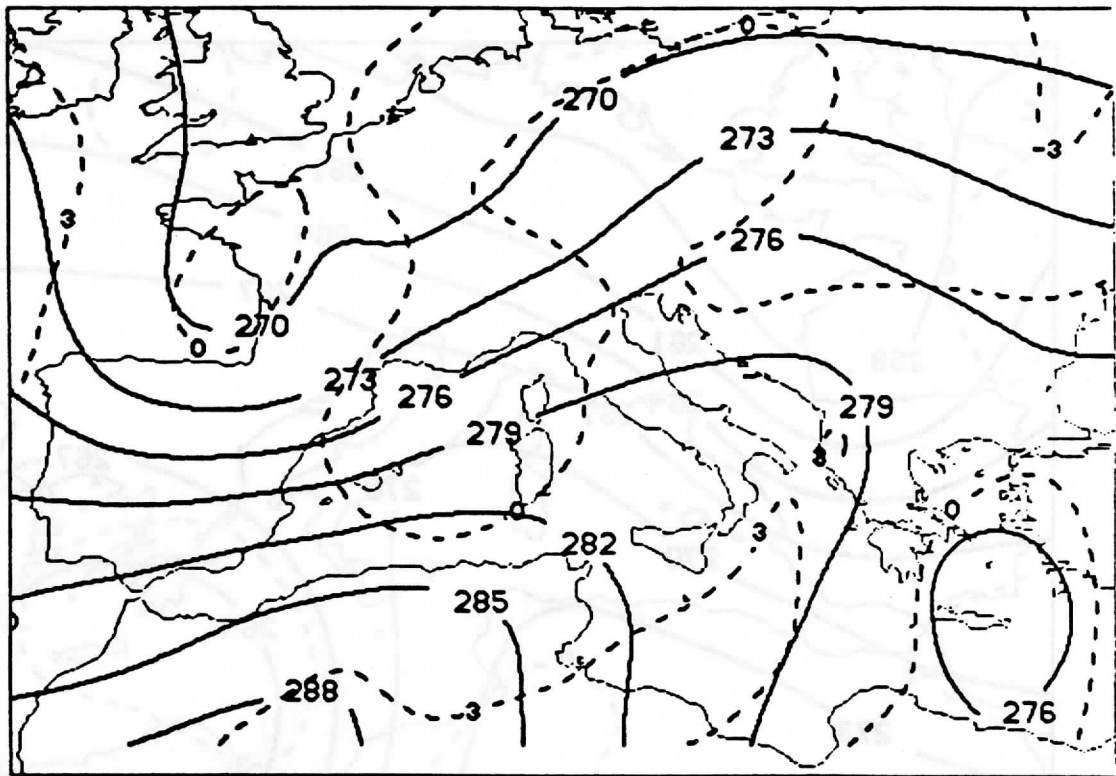


5 MARCH 1982 0000GMT
850MB T(K)

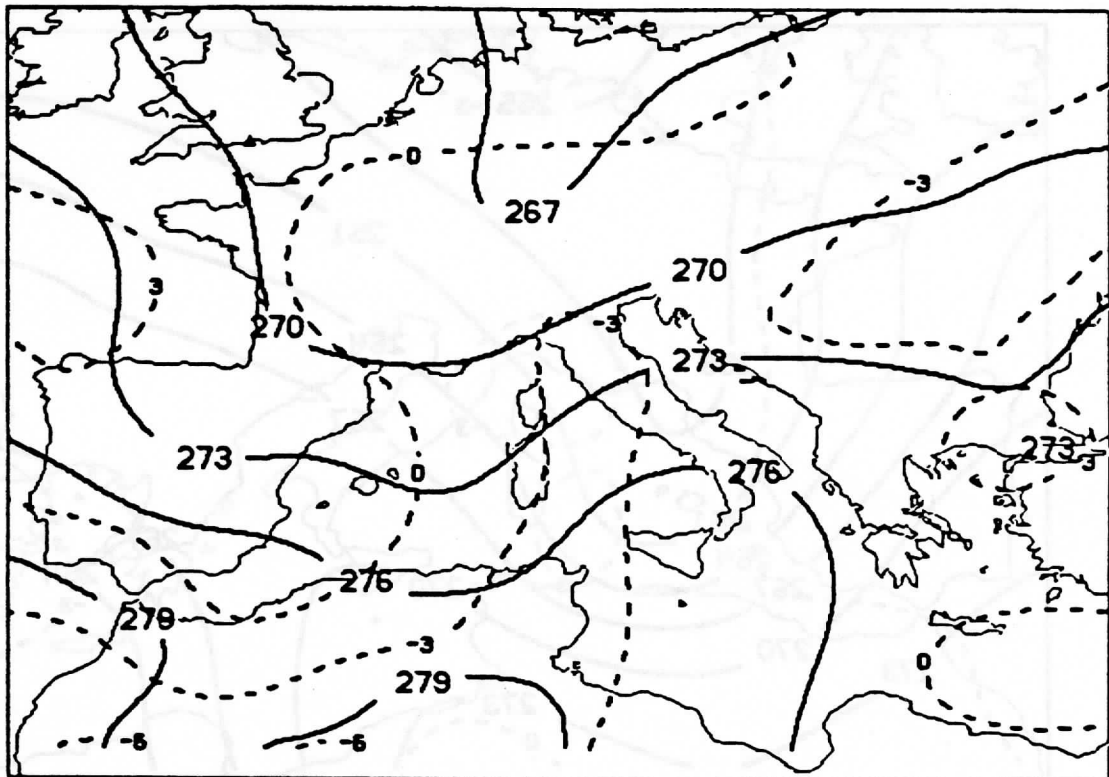
REGRESSION
SAT ANAL(SOLID) ECMWF - SAT ANAL(DASHED)

(c)

Figure 1: Analyses of TOVS retrievals (solid contours) and differences between the operational analyses of the ECMWF and the TOVS analyses (dashed contours).

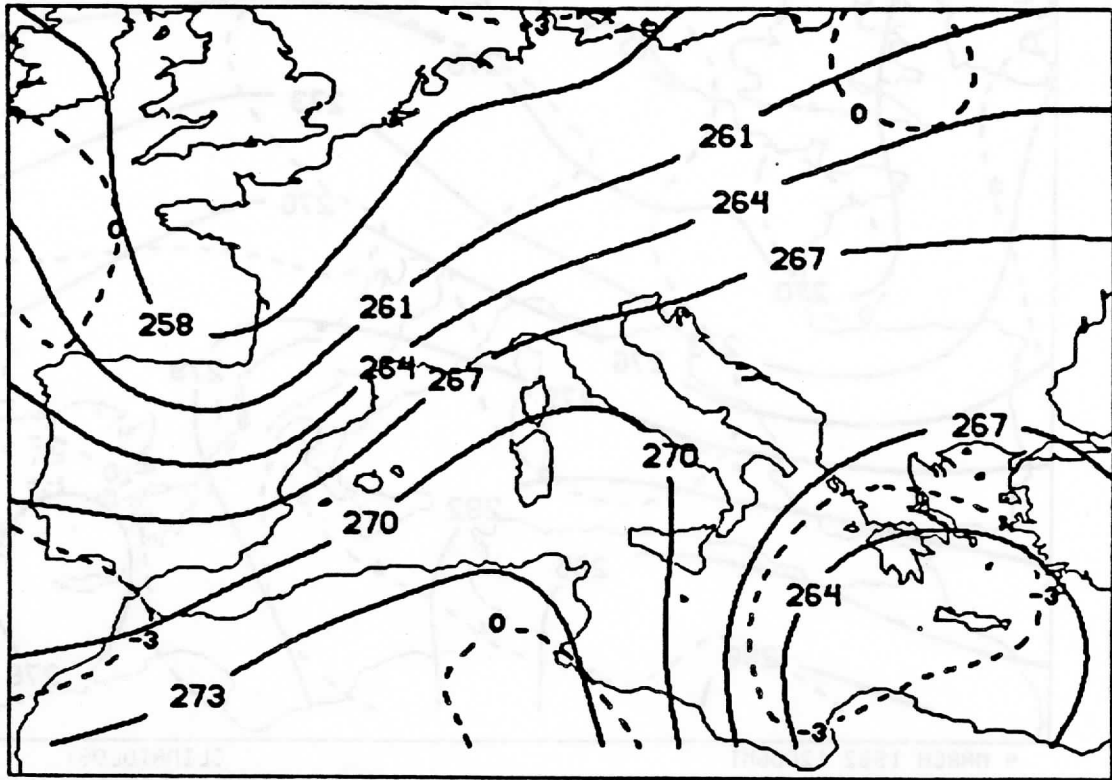


(b) 4 MARCH 1982 1200GMT
 850MB T(K) SAT ANAL (SOLID) CLIMATOLOGY
 ECMWF - SAT ANAL (DASHED)



(d) 5 MARCH 1982 0000GMT
 850MB T(K) SAT ANAL (SOLID) CLIMATOLOGY
 ECMWF - SAT ANAL (DASHED)

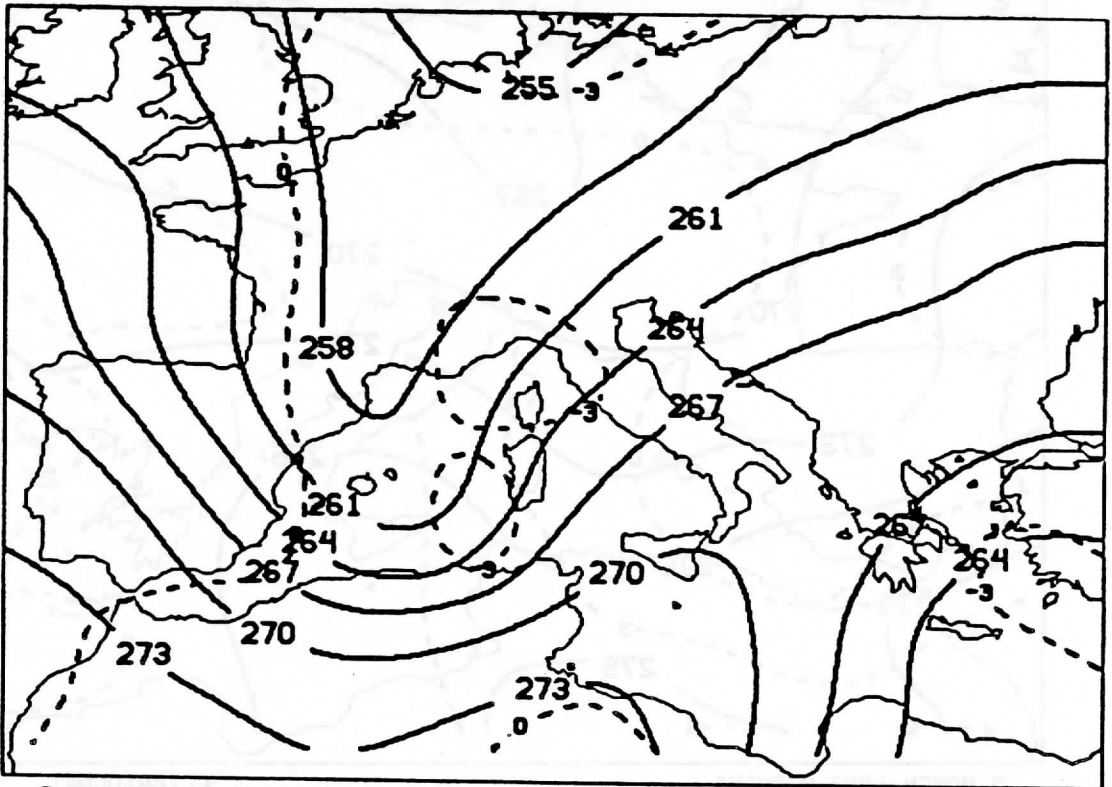
Figure 1: Analyses of TOVS retrievals (solid contours) and differences between the operational analyses of the ECMWF and the TOVS analyses (dashed contours).



4 MARCH 1982 1200GMT
700MB T(K)

SAT ANAL (SOLID) REGRESSION
ECMWF - SAT ANAL (DASHED)

(a)

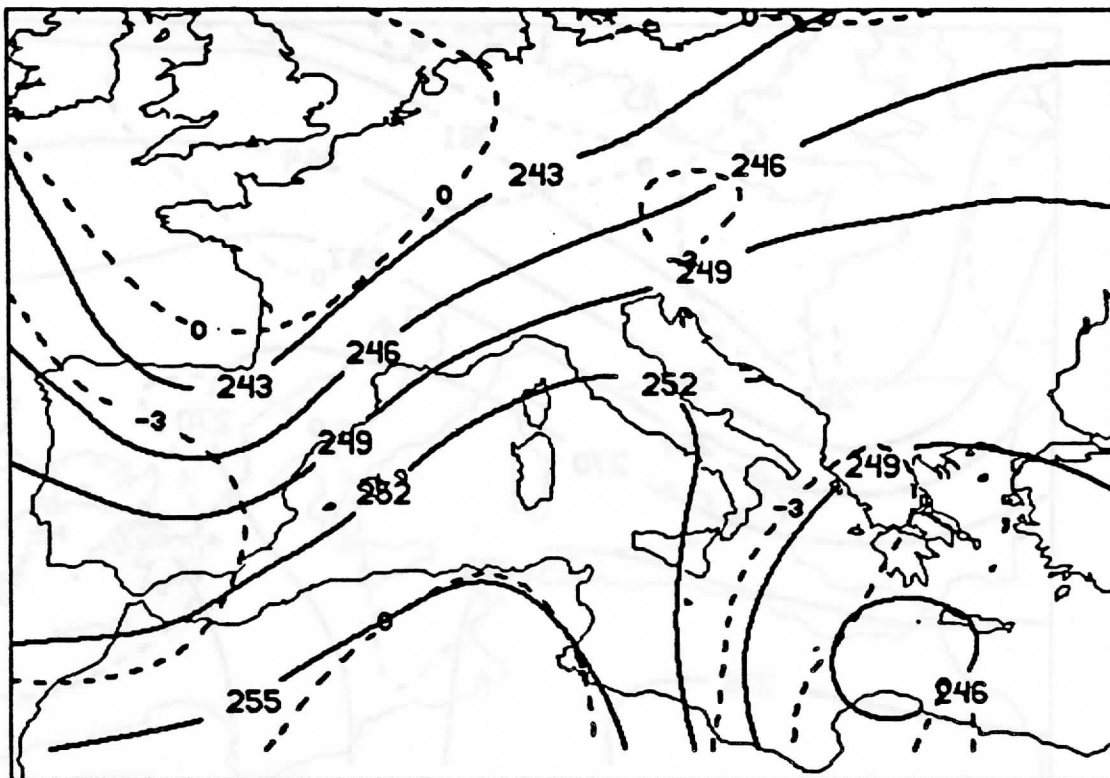


5 MARCH 1982 0000GMT
700MB T(K)

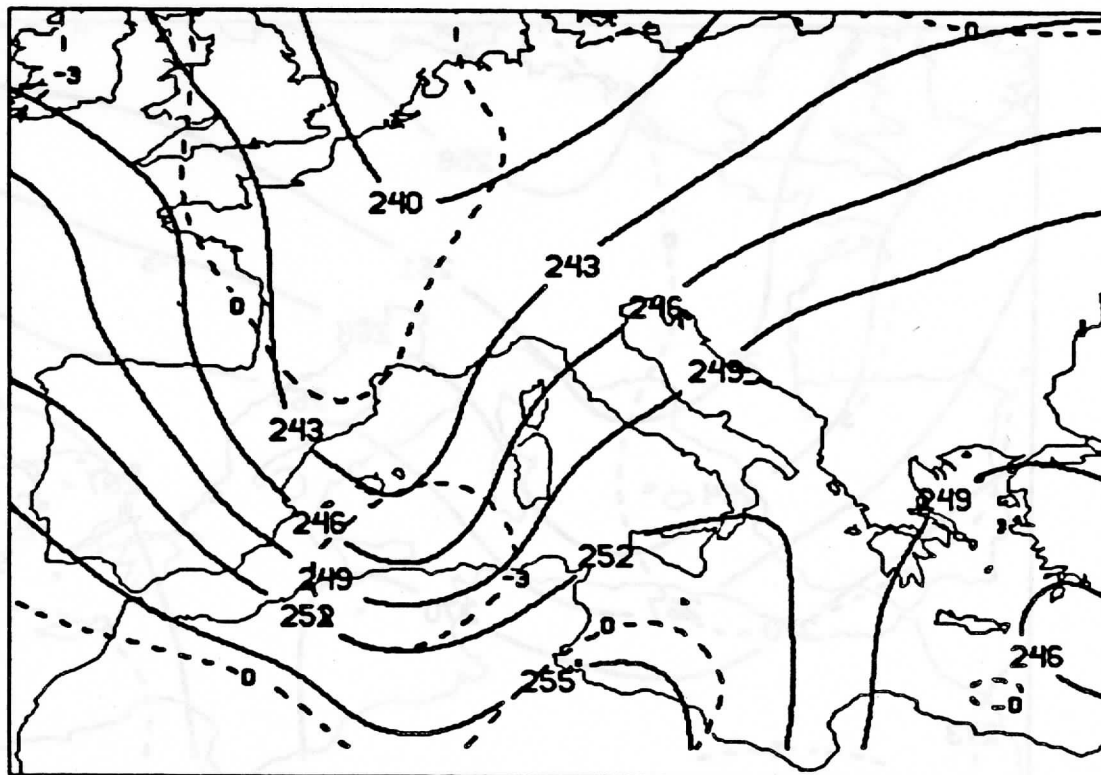
SAT ANAL (SOLID) REGRESSION
ECMWF - SAT ANAL (DASHED)

(c)

Figure 2: Analyses of TOVS retrievals (solid contours) and differences between the operational analyses of the ECMWF and the TOVS analyses (dashed contours).

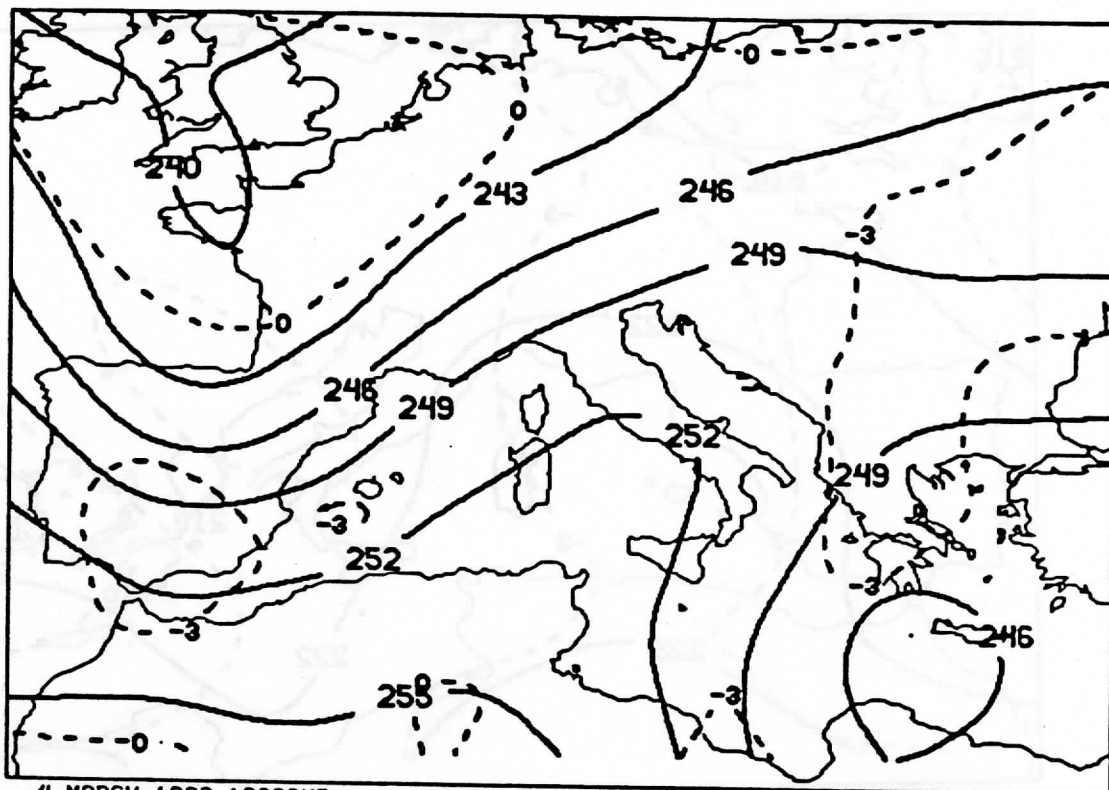


(a) 4 MARCH 1982 1200GMT
 500MB T(K) REGRESSION
 SAT ANAL(SOLID) ECMWF - SAT ANAL(DASHED)



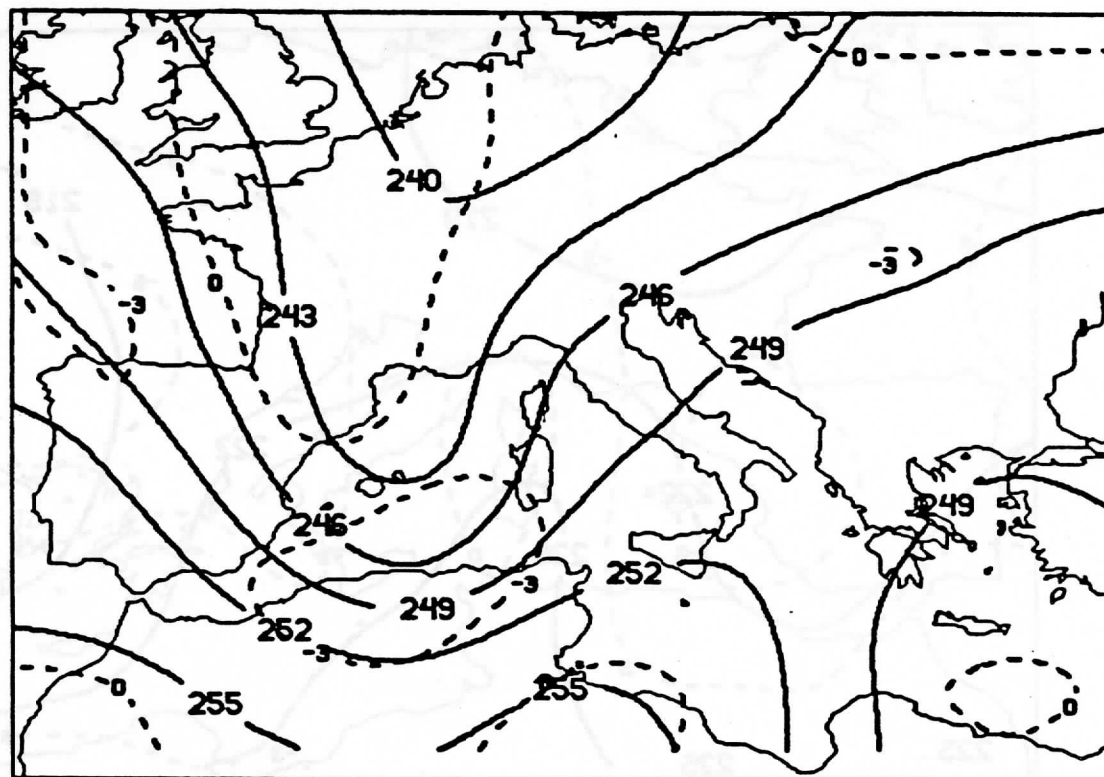
(c) 5 MARCH 1982 0000GMT
 500MB T(K) REGRESSION
 SAT ANAL(SOLID) ECMWF - SAT ANAL(DASHED)

Figure 3: Analyses of TOVS retrievals (solid contours) and differences between the operational analyses of the ECMWF and the TOVS analyses (dashed contours).



(b) 4 MARCH 1982 1200GMT
500MB T(K)

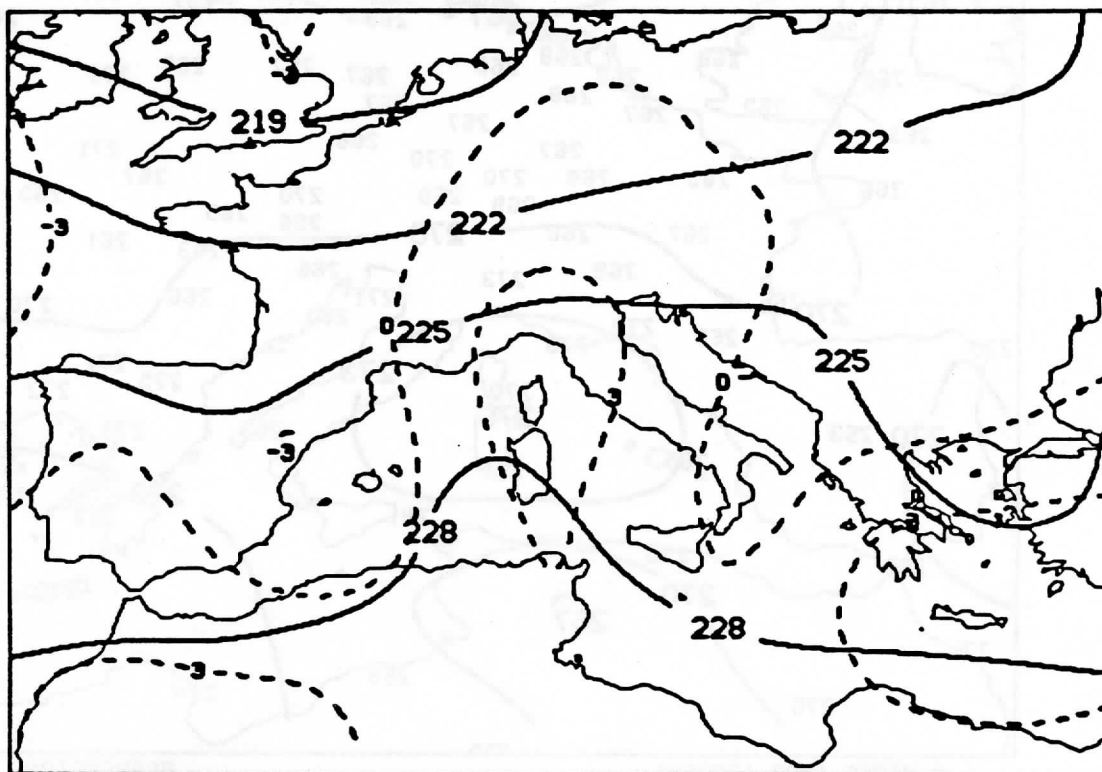
SAT ANAL(SOLID) CLIMATOLOGY
ECMWF - SAT ANAL(DASHED)



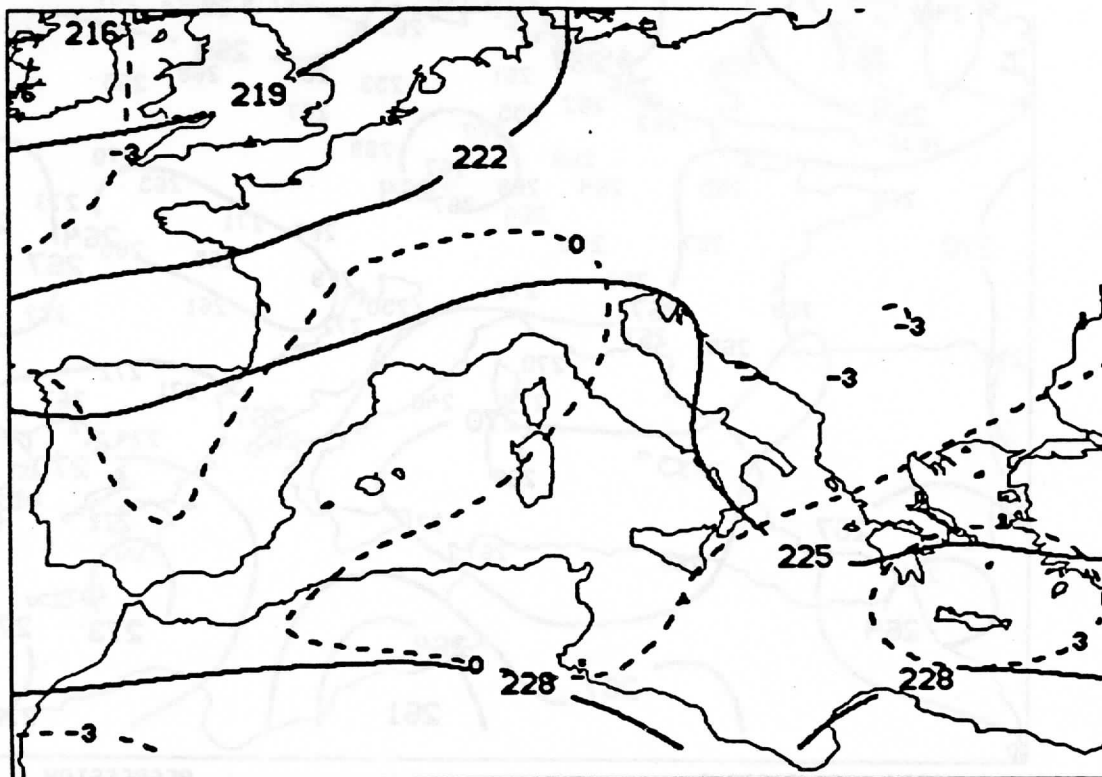
(d) 5 MARCH 1982 0000GMT
500MB T(K)

SAT ANAL(SOLID) CLIMATOLOGY
ECMWF - SAT ANAL(DASHED)

Figure 3: Analyses of TOVS retrievals (solid contours) and differences between the operational analyses of the ECMWF and the TOVS analyses (dashed contours).

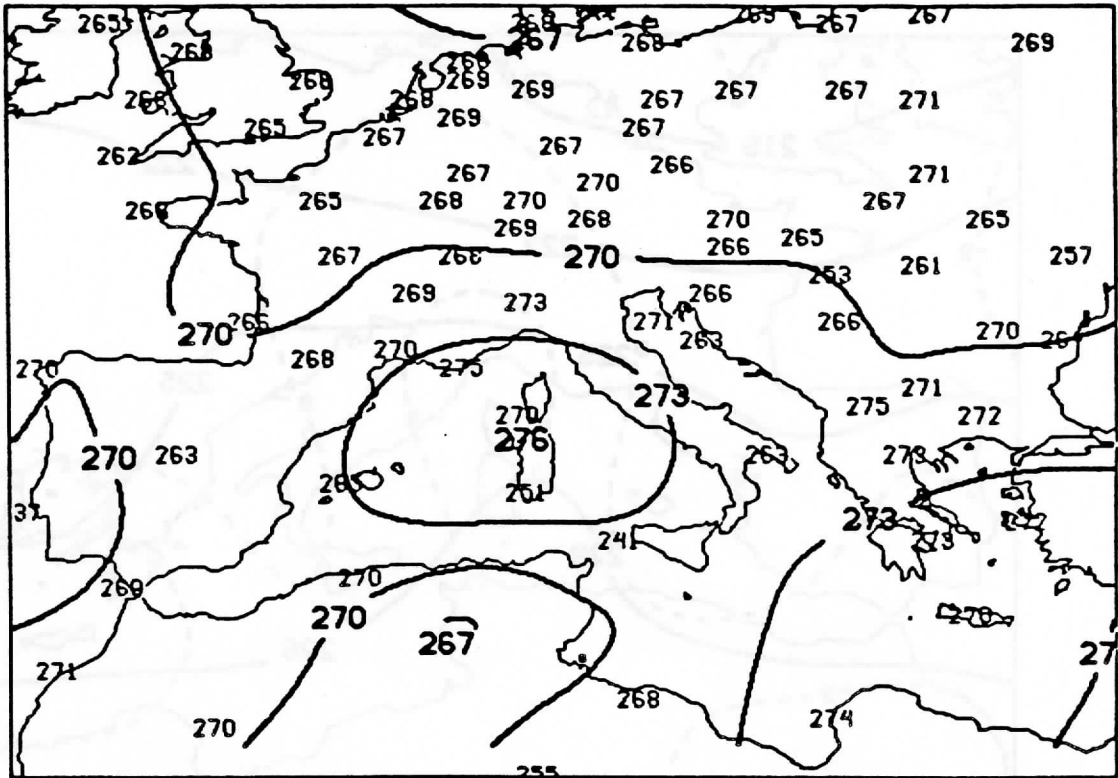


(b) 5 MARCH 1982 0000GMT
 300MB T(K) SAT ANAL(SOLID) CLIMATOLOGY
 ECMWF - SAT ANAL(DASHED)

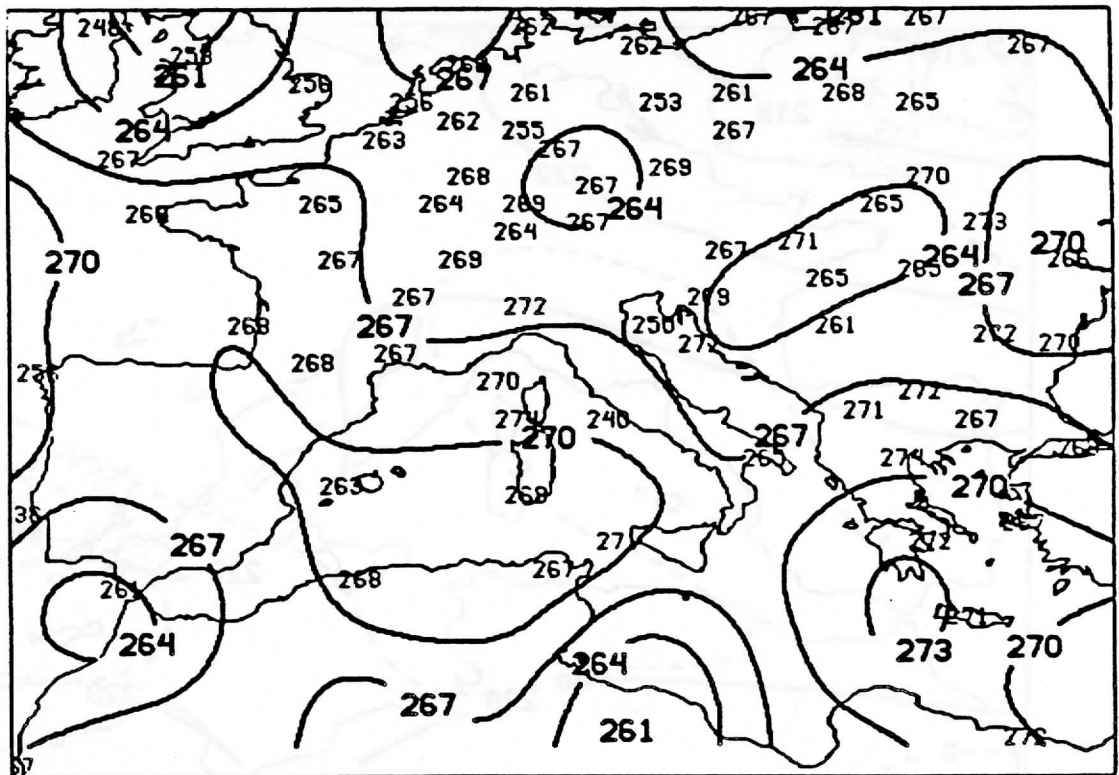


(d) 4 MARCH 1982 1200GMT
 300MB T(K) SAT ANAL(SOLID) CLIMATOLOGY
 ECMWF - SAT ANAL(DASHED)

Figure 4: Analyses of TOVS retrievals (solid contours) and differences between the operational analyses of the ECMWF and the TOVS analyses (dashed contours).

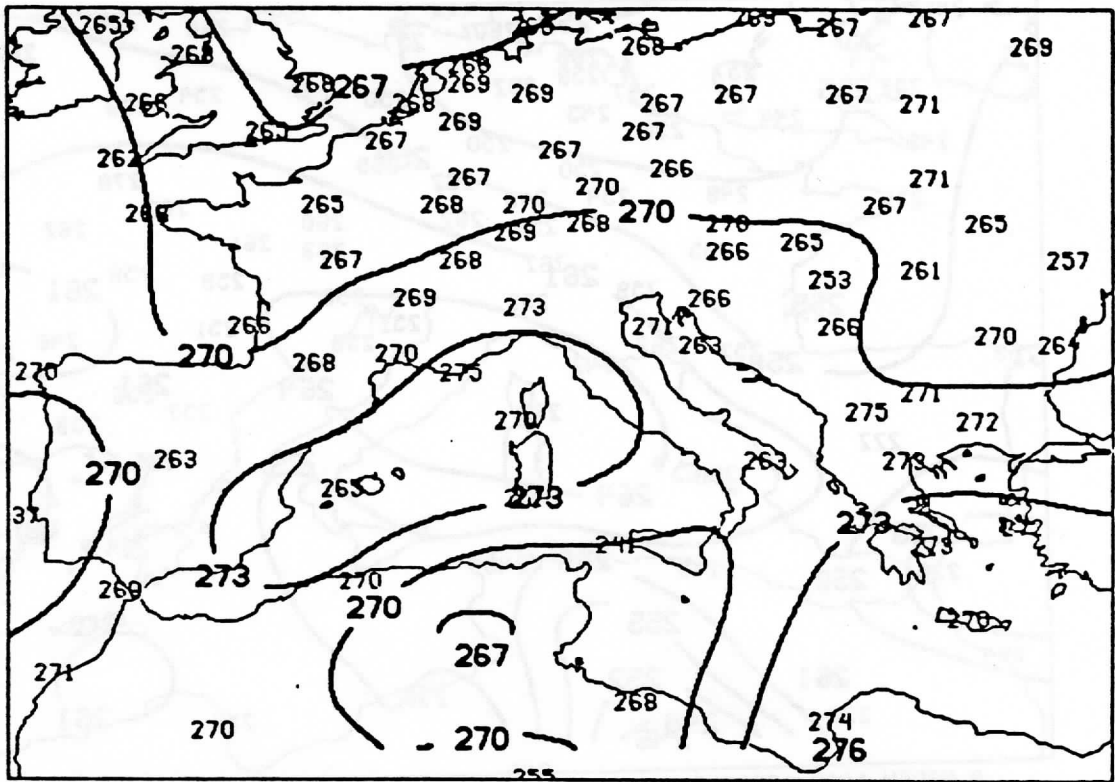


(a) 4 MARCH 1982 1200GMT REGRESSION SAT ANAL RAOB PLOTTED

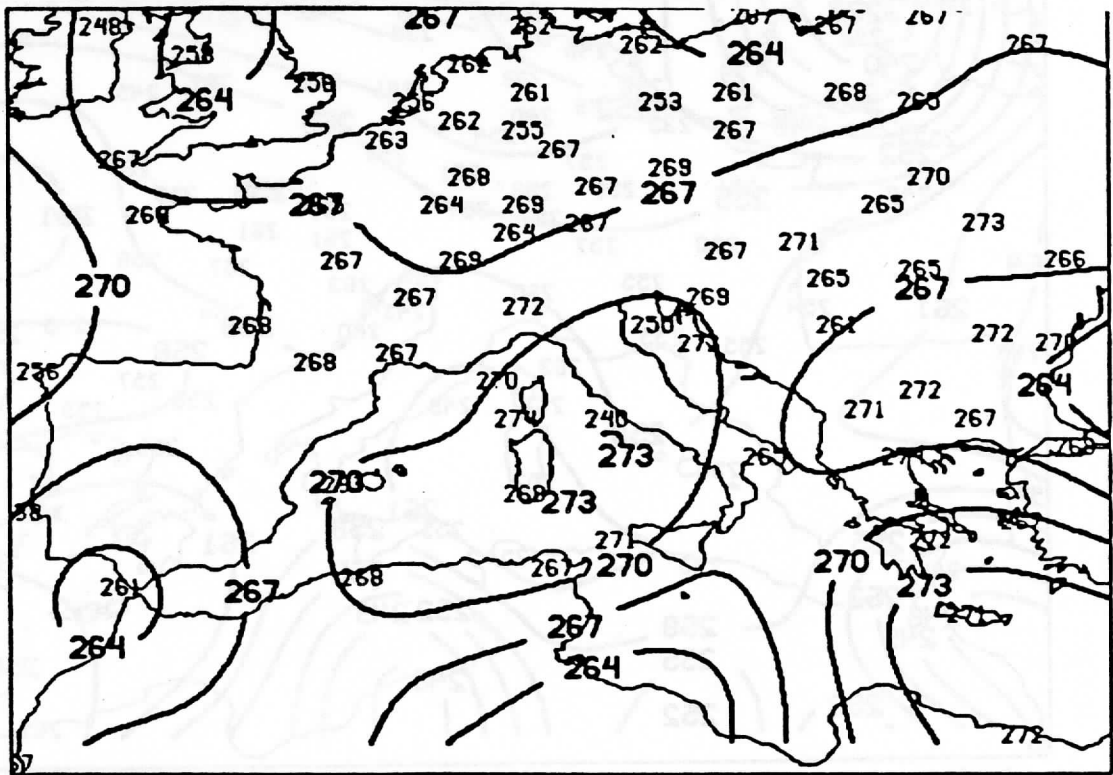


(c) 5 MARCH 1982 0000GMT REGRESSION SAT ANAL RAOB PLOTTED

Figure 5: Analyses of TOVS retrievals (solid contours).

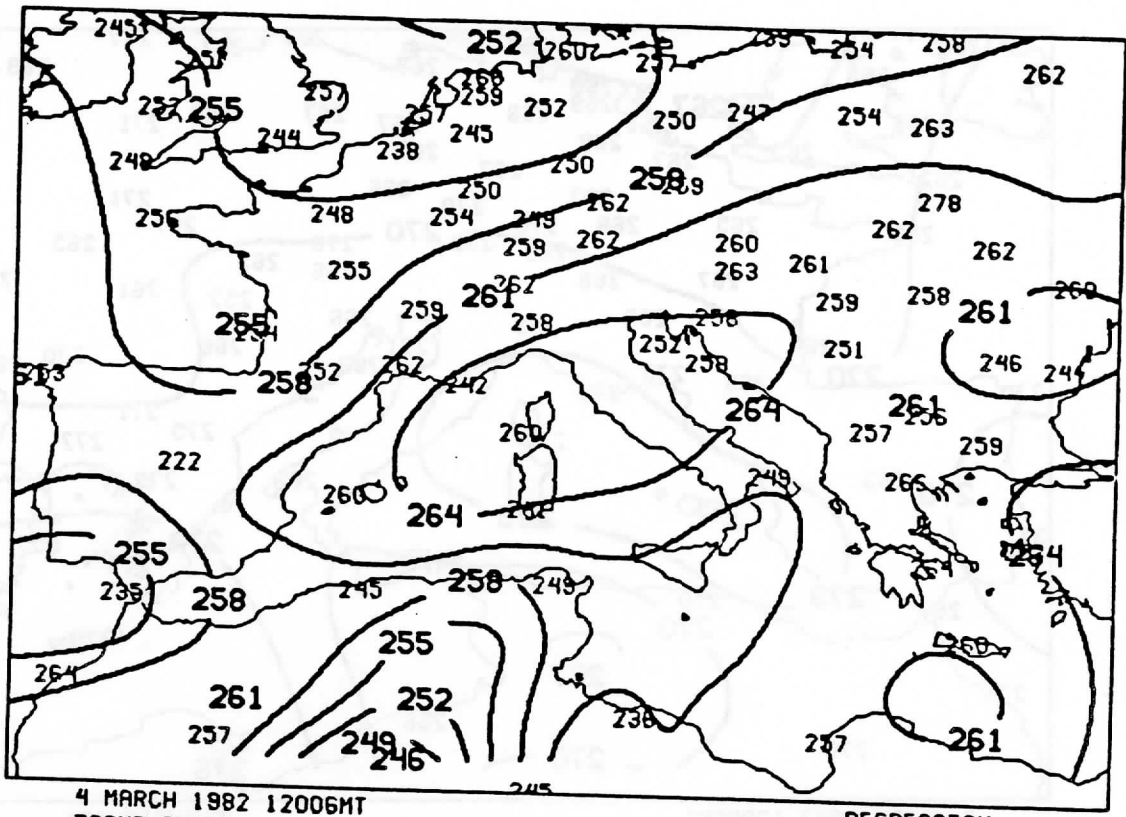


(b) 4 MARCH 1982 1200GMT CLIMATOLOGY
 850MB TD(K) SAT ANAL RAOB PLOTTED



(d) 5 MARCH 1982 0000GMT CLIMATOLOGY
 850MB TD(K) SAT ANAL RAOB PLOTTED

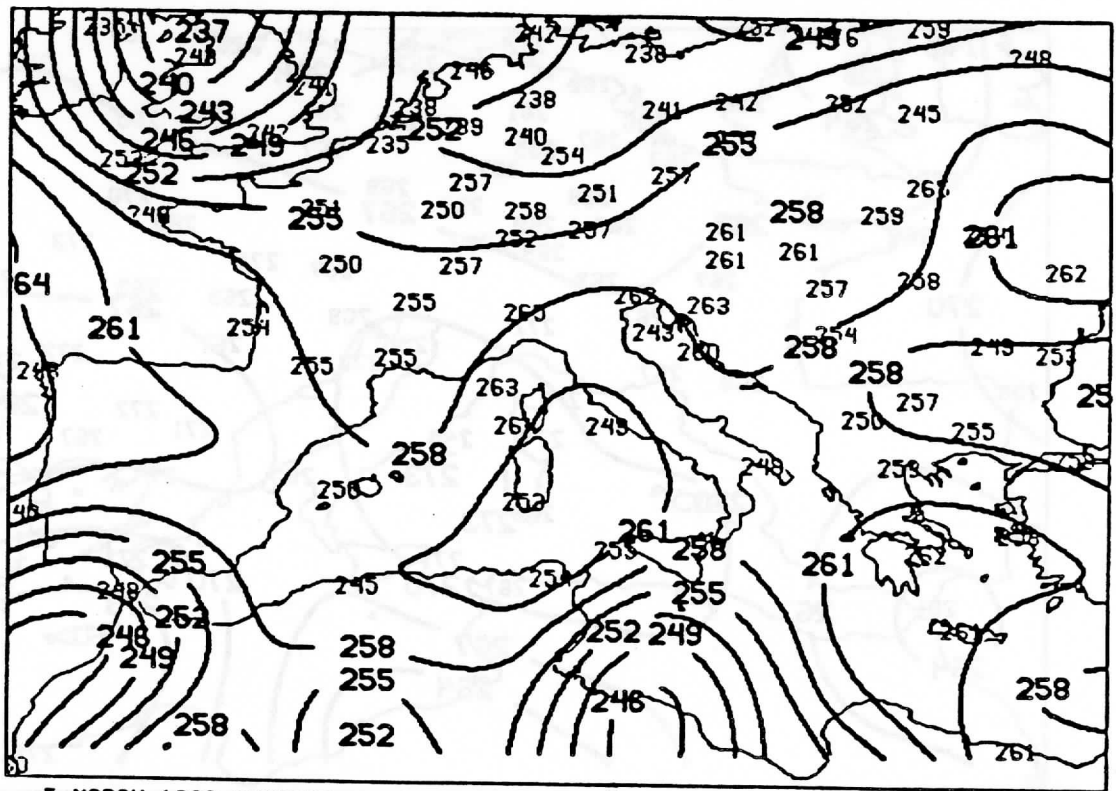
Figure 5: Analyses of TOVS retrievals (solid contours).



(a)

4 MARCH 1982 1200GMT
700MB TD(K)

REGRESSION
SAT ANAL
RAOB PLOTTED

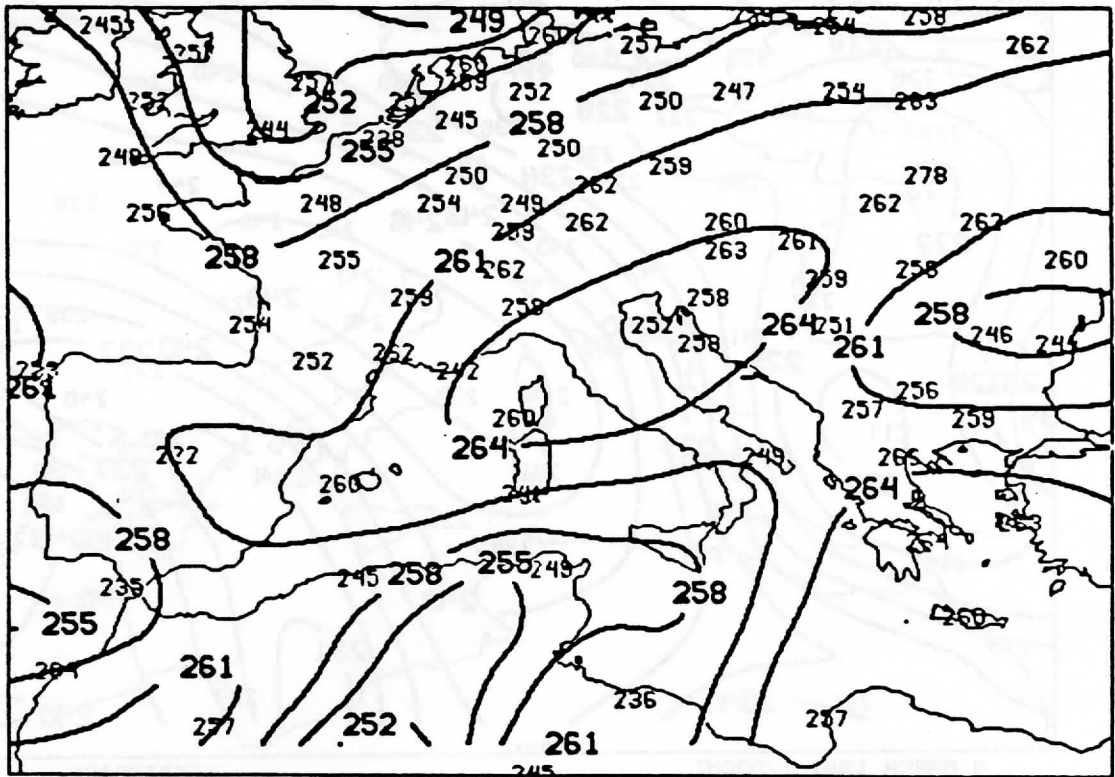


(c)

5 MARCH 1982 0000GMT
700MB TD(K)

REGRESSION
SAT ANAL
RAOB PLOTTED

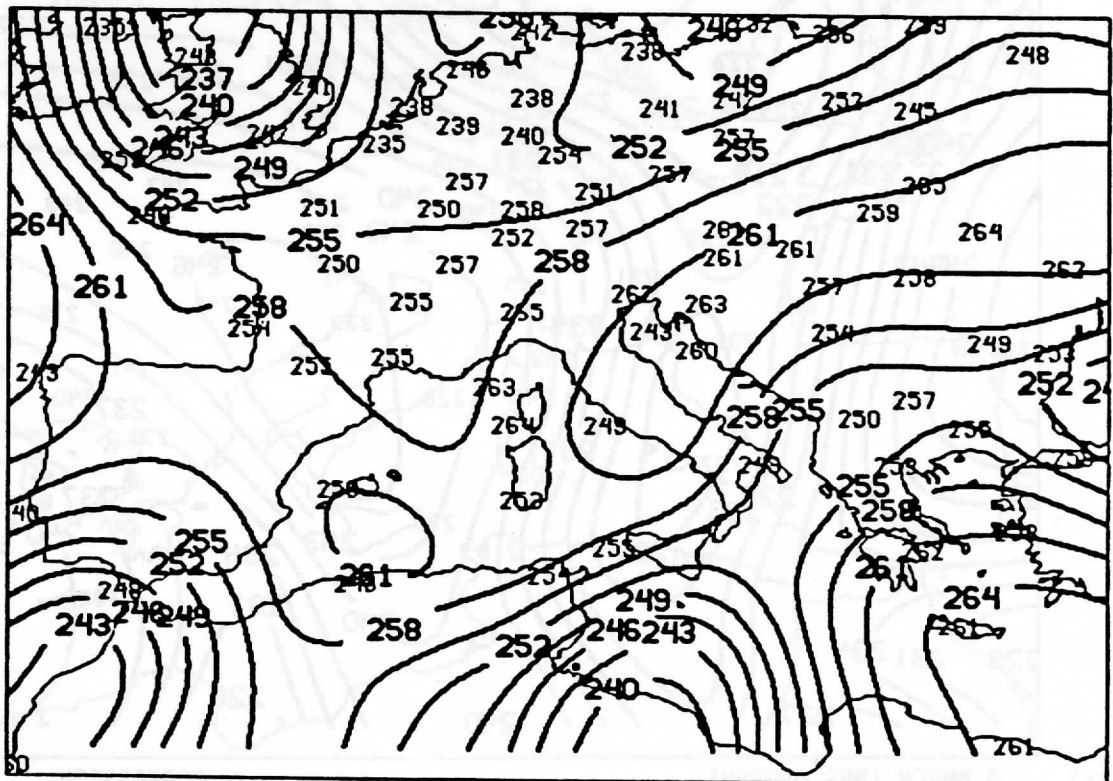
Figure 6: Analyses of TOVS retrievals (solid contours).



(b)

4 MARCH 1982 1200GMT
700MB TD(K)

CLIMATOLOGY
SAT ANAL RAOB PLOTTED

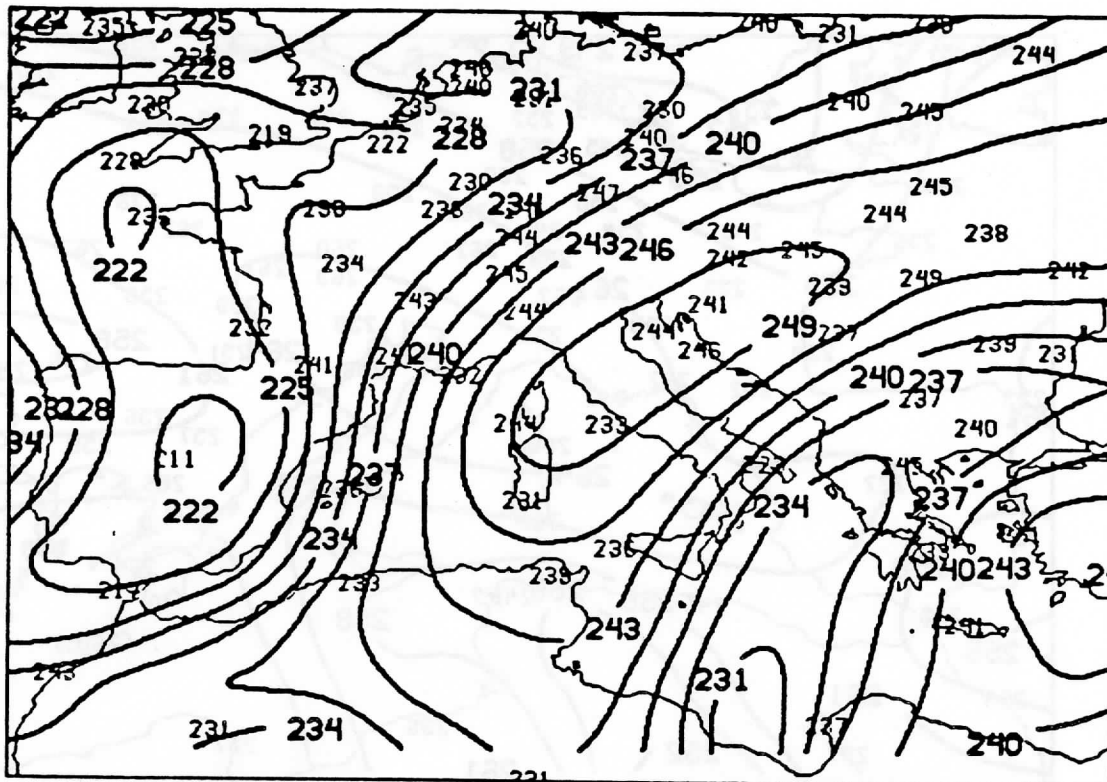


(d)

5 MARCH 1982 0000GMT
700MB TD(K)

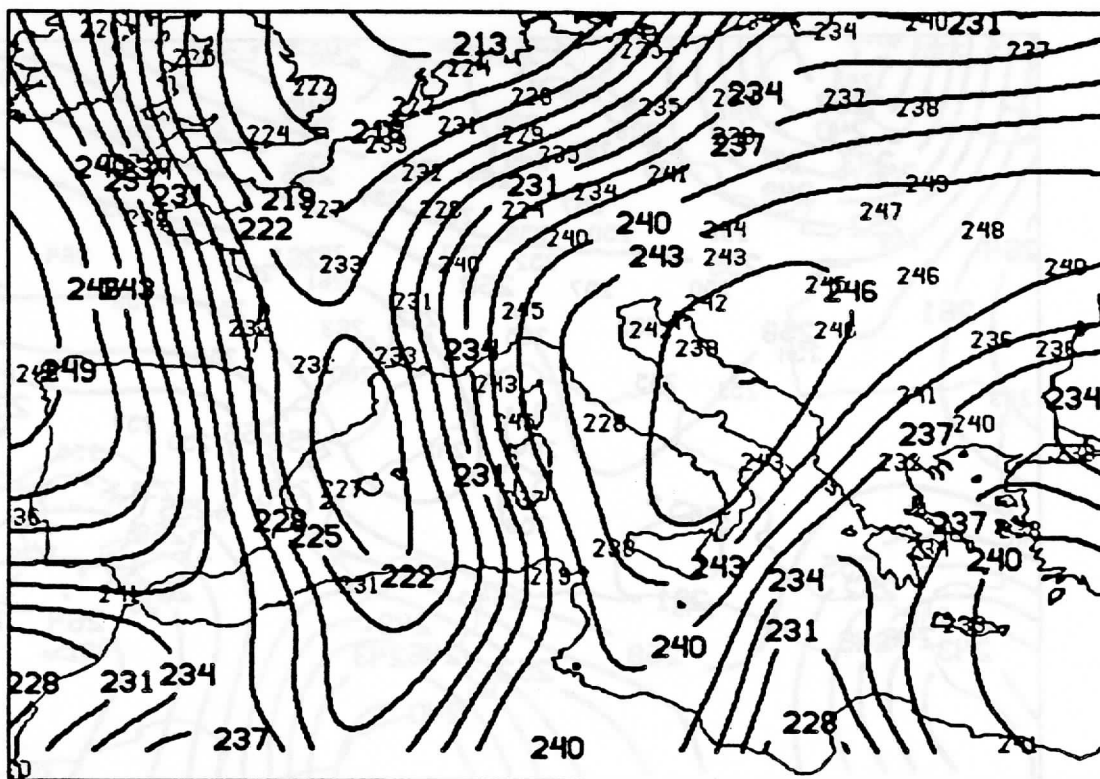
CLIMATOLOGY
SAT ANAL RAOB PLOTTED

Figure 6: Analyses of TOVS retrievals (solid contours).



(a) 4 MARCH 1982 1200GMT
500MB TD(K)

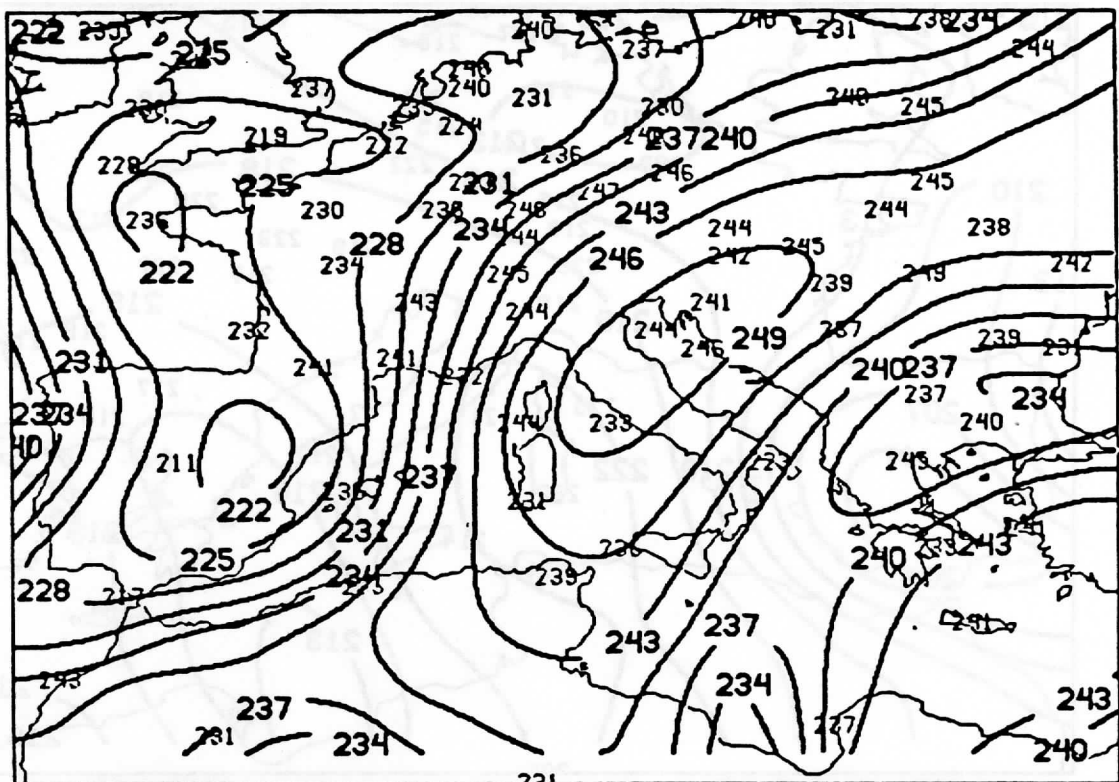
REGRESSION
SAT ANAL RAOB PLOTTED



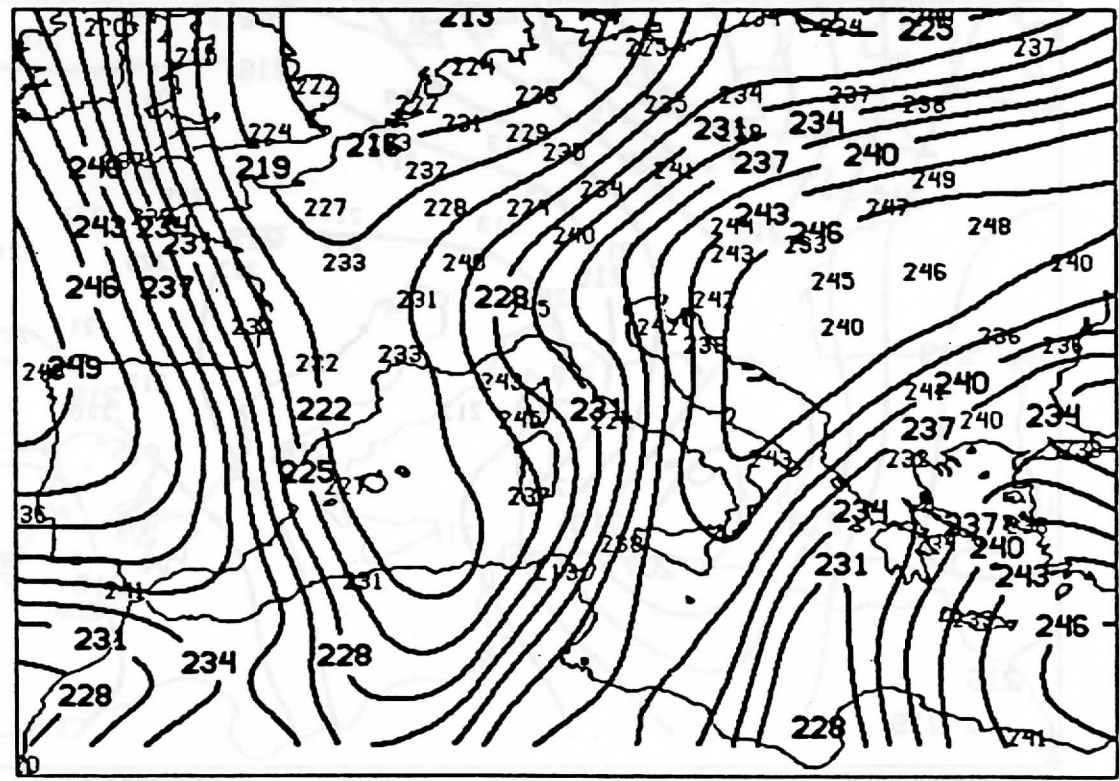
(c) 5 MARCH 1982 0000GMT
500MB TD(K)

REGRESSION
SAT ANAL RAOB PLOTTED

Figure 7: Analyses of TOVS retrievals (solid contours).

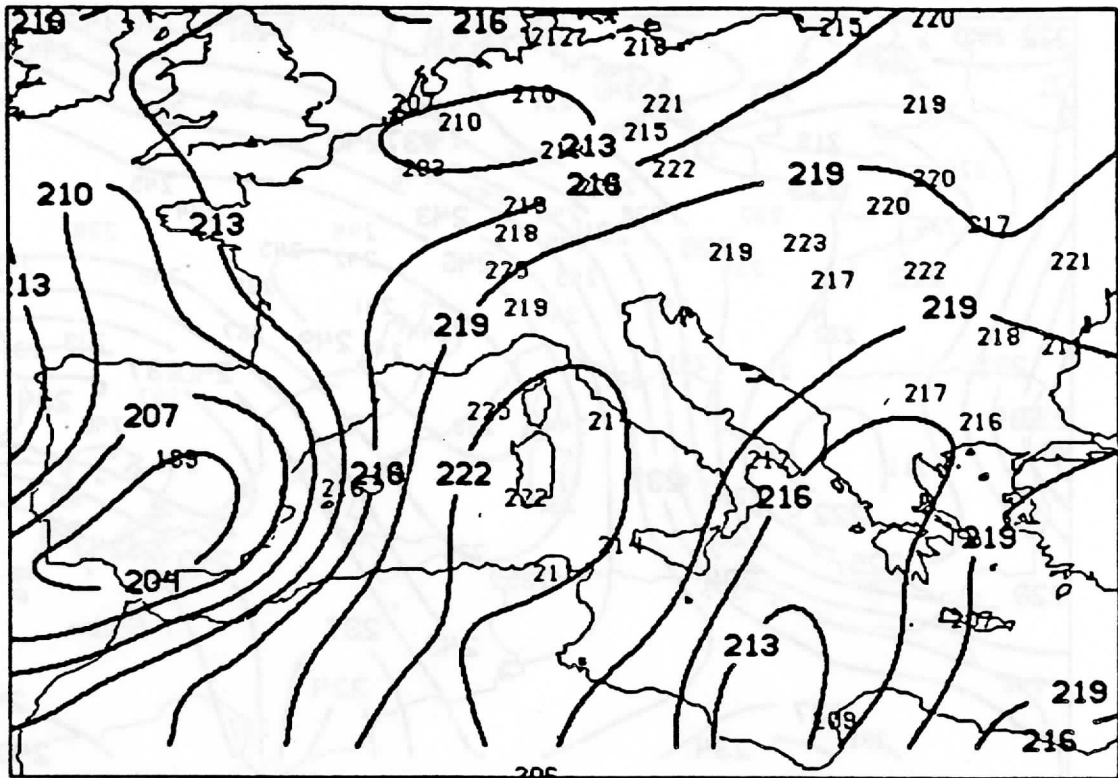


(b) 4 MARCH 1982 1200GMT CLIMATOLOGY
 500MB TD(K) SAT ANAL RAOB PLOTTED



(d) 5 MARCH 1982 0000GMT CLIMATOLOGY
 500MB TD(K) SAT ANAL RAOB PLOTTED

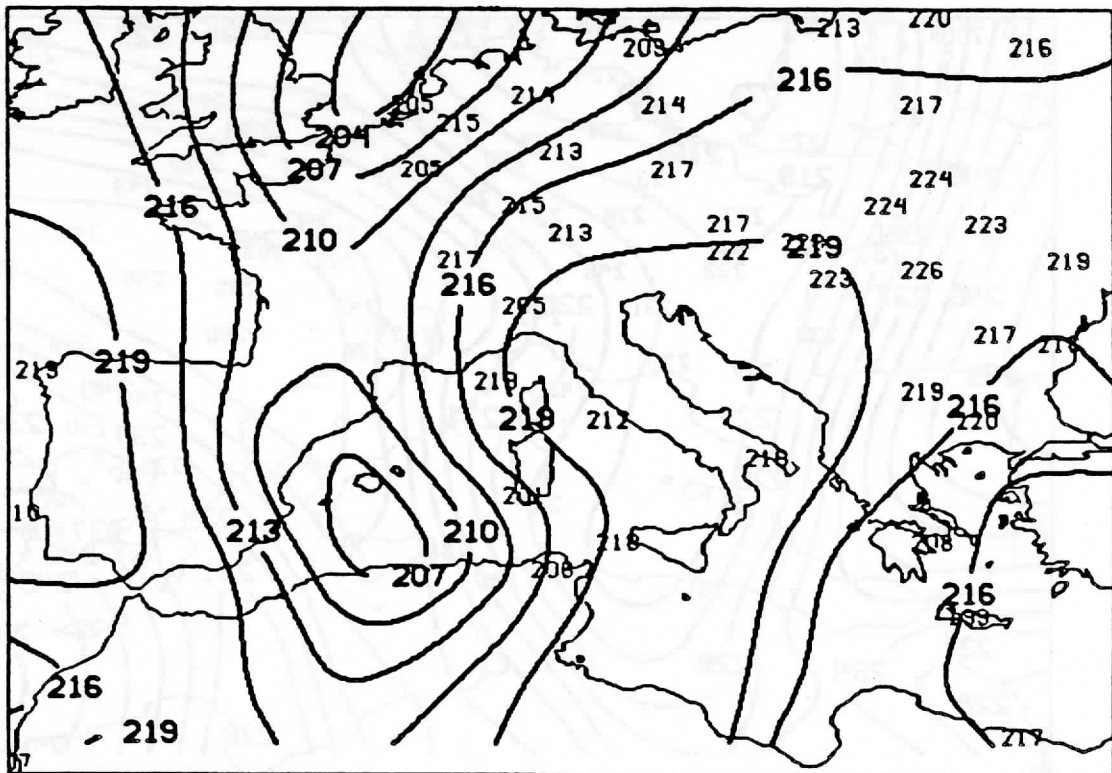
Figure 7: Analyses of TOVS retrievals (solid contours).



4 MARCH 1982 1200GMT
300MB TD(K)

REGRESSION
SAT ANAL RAOB PLOTTED

(a)

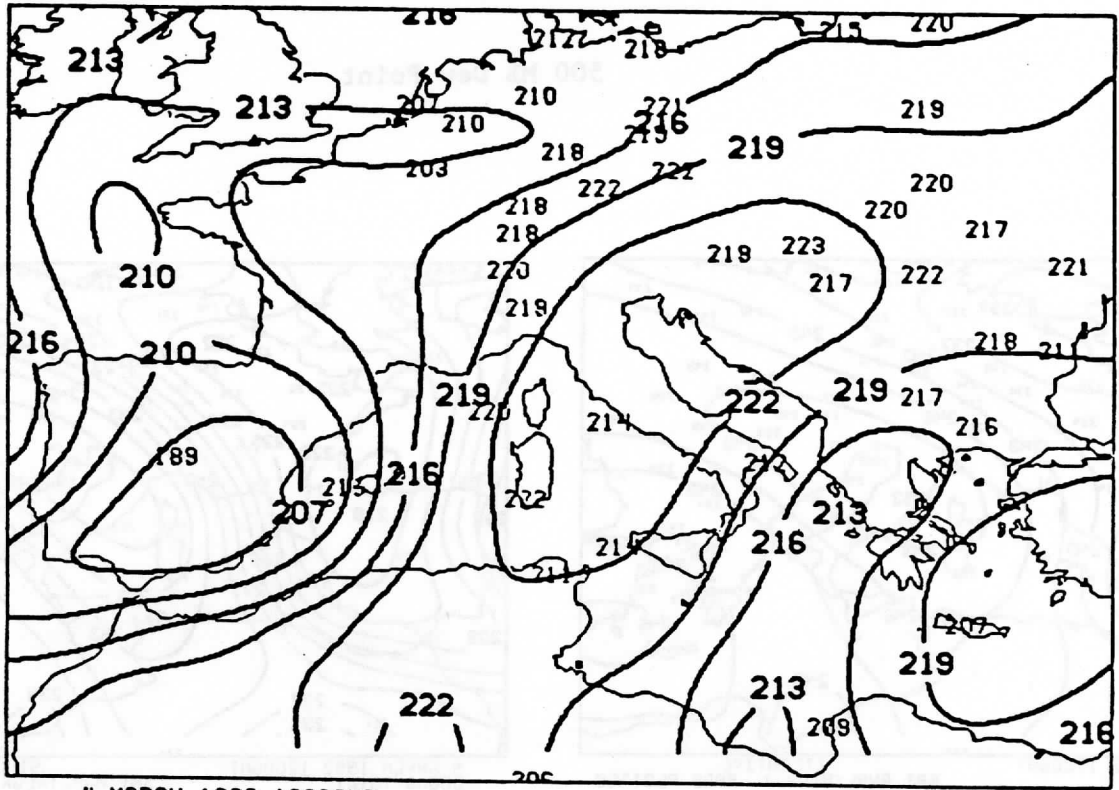


5 MARCH 1982 0000GMT
300MB TD(K)

REGRESSION
SAT ANAL RAOB PLOTTED

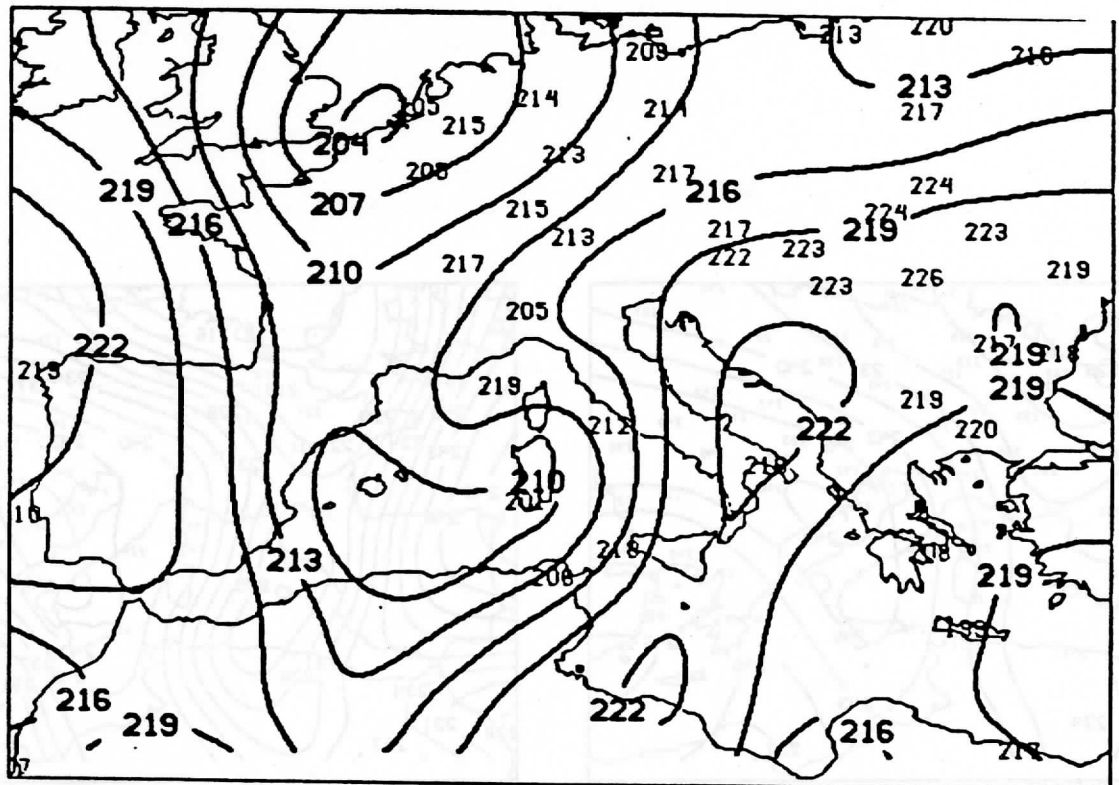
(c)

Figure 8: Analyses of TOVS retrievals (solid contours).



(b) 4 MARCH 1982 1200GMT
300MB TD(K)

CLIMATOLOGY
SAT ANAL RAOB PLOTTED

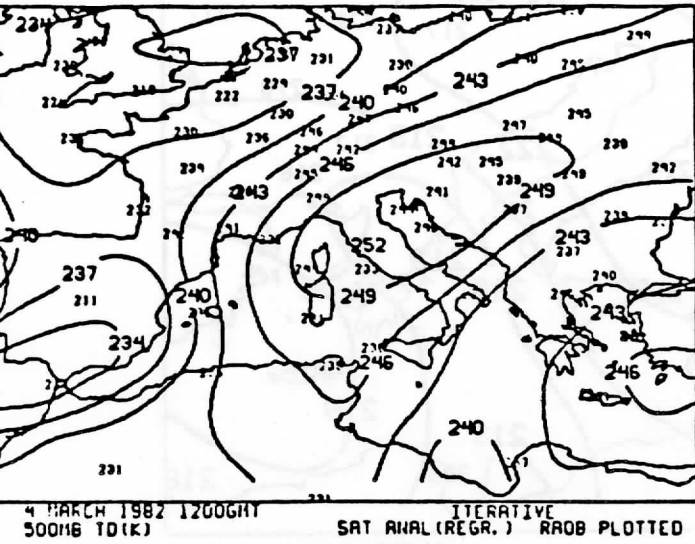


(d) 5 MARCH 1982 0000GMT
300MB TD(K)

CLIMATOLOGY
SAT ANAL RAOB PLOTTED

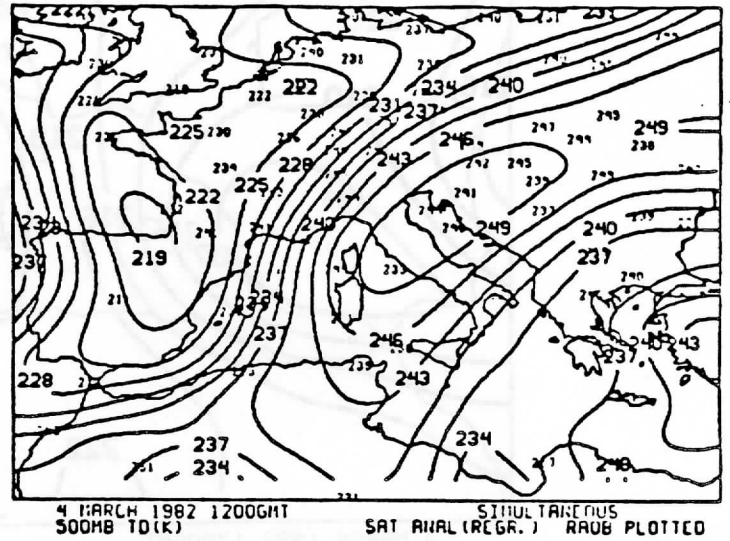
Figure 8: Analyses of TOVS retrievals (solid contours).

500 MB Dew Point



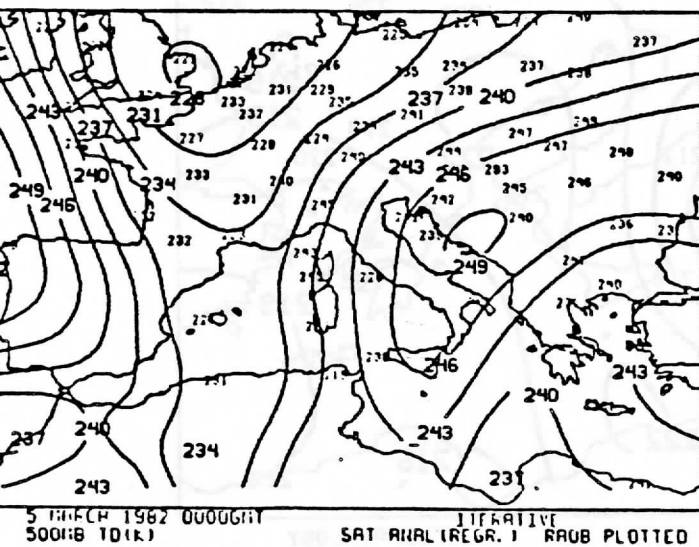
Simultaneous

Mar 4



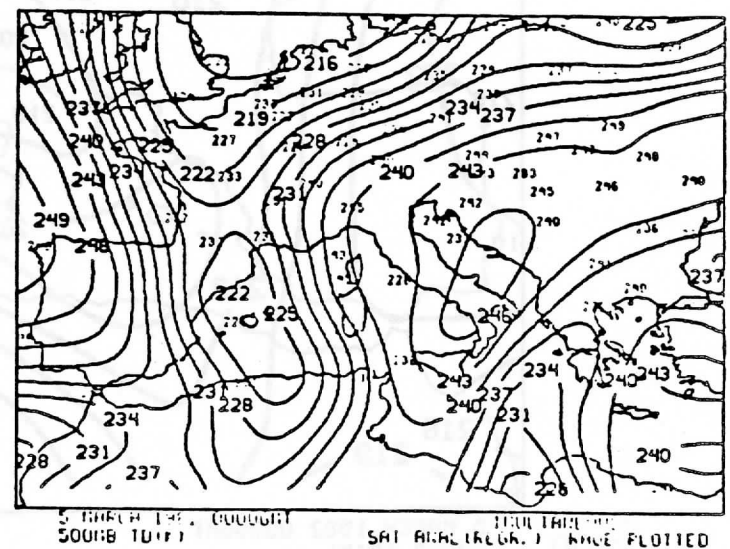
Iterative

Mar 4



Simultaneous

Mar 5



Iterative

Mar 5

Figure 9

RAOB VS ECMWF
MARCH 4&5, 1982

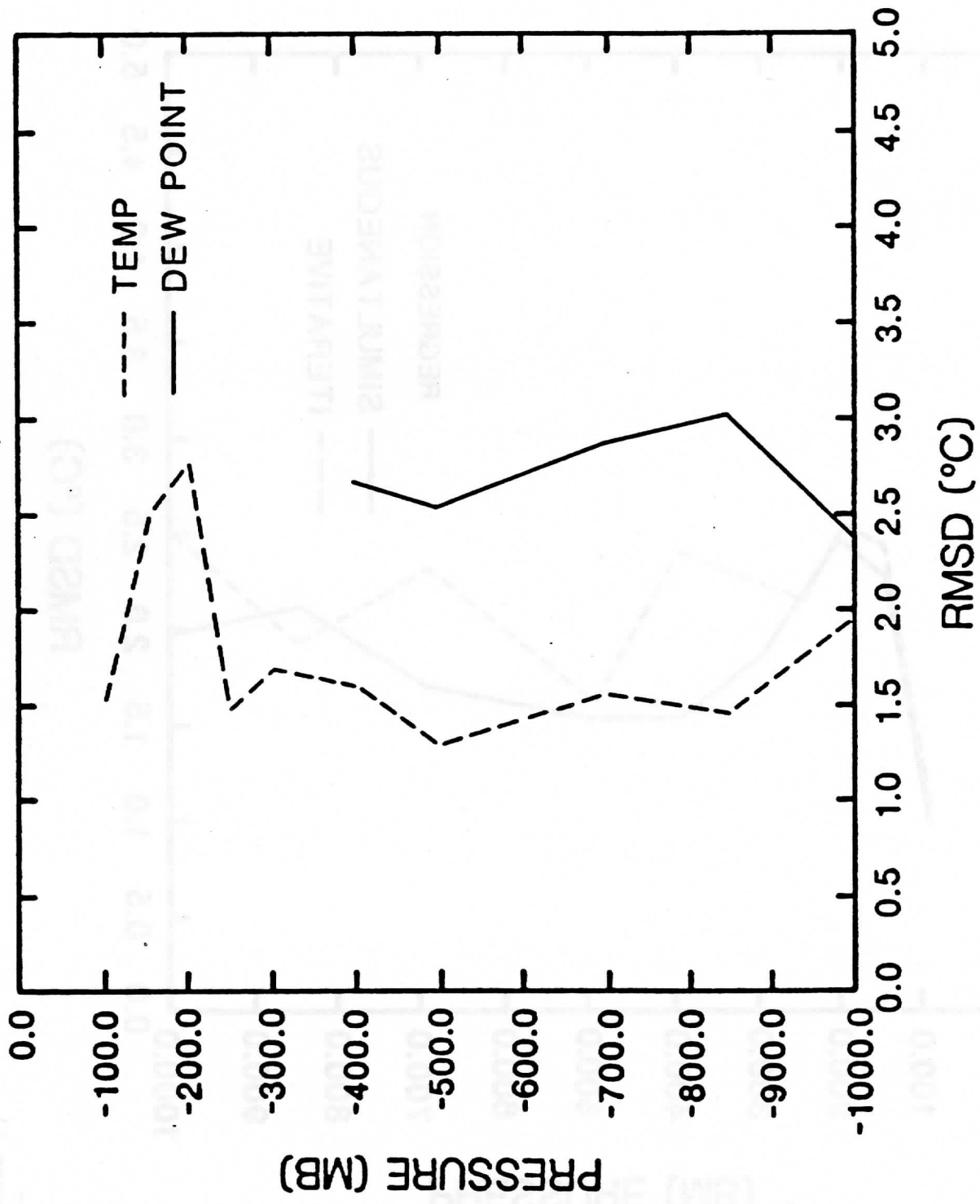


Figure 10

RETRIEVALS VS. ECMWF MARCH 4&5, 1982

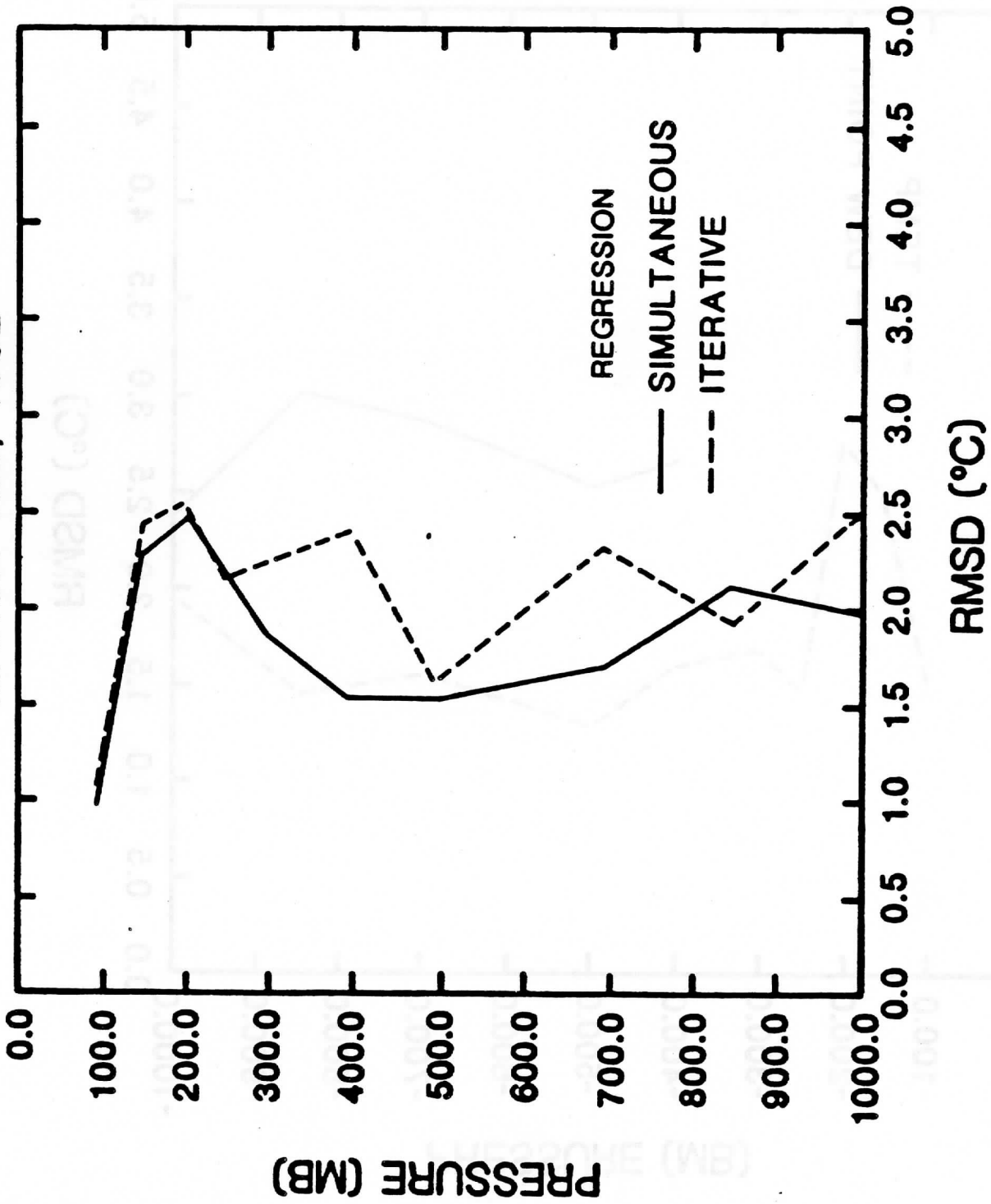


Figure 11

RETRIEVALS VS. ECMWF MARCH 4&5, 1982

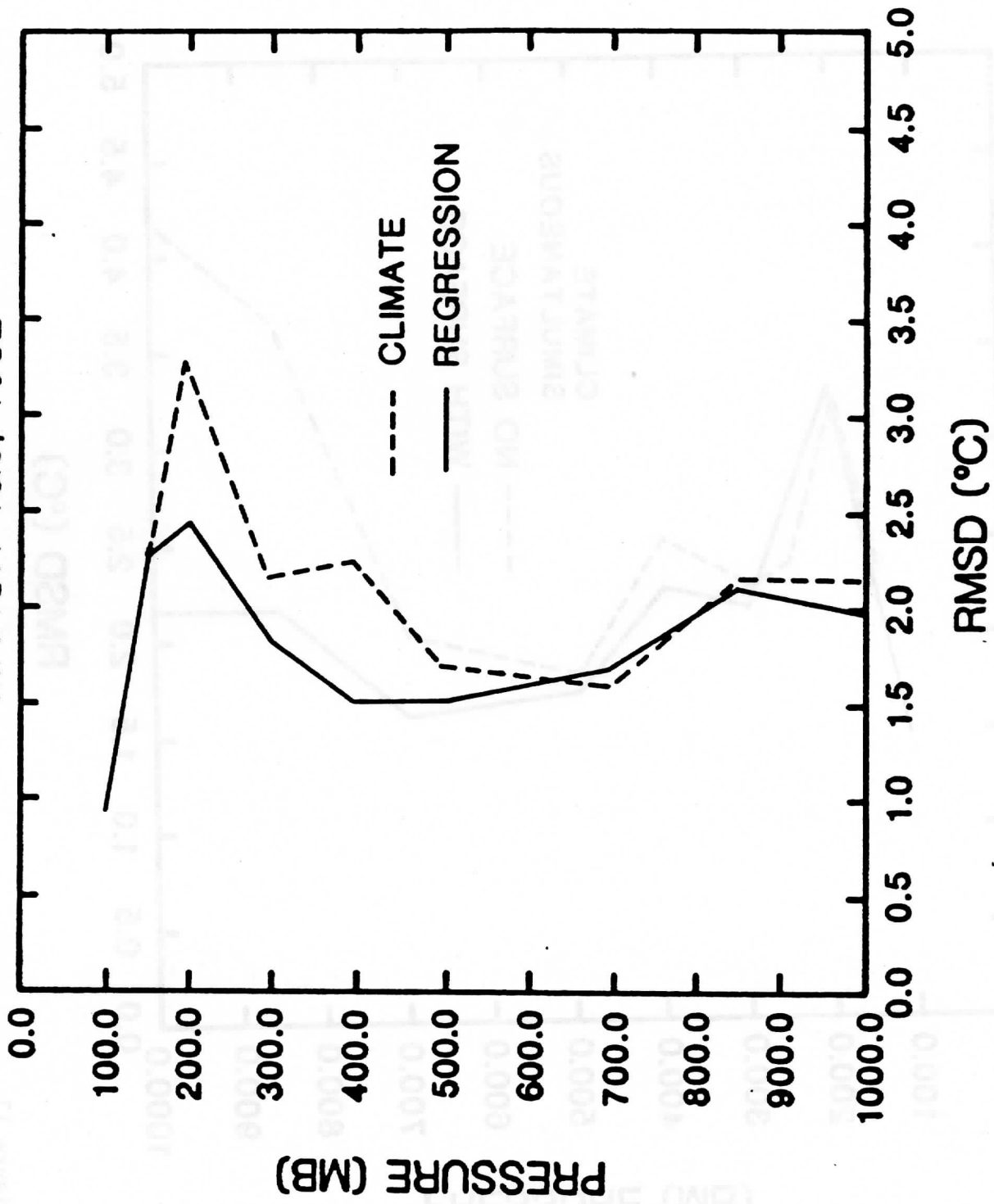


Figure 12

RETRIEVALS VS. ECMWF (TEMP)
MARCH 4&5, 1982

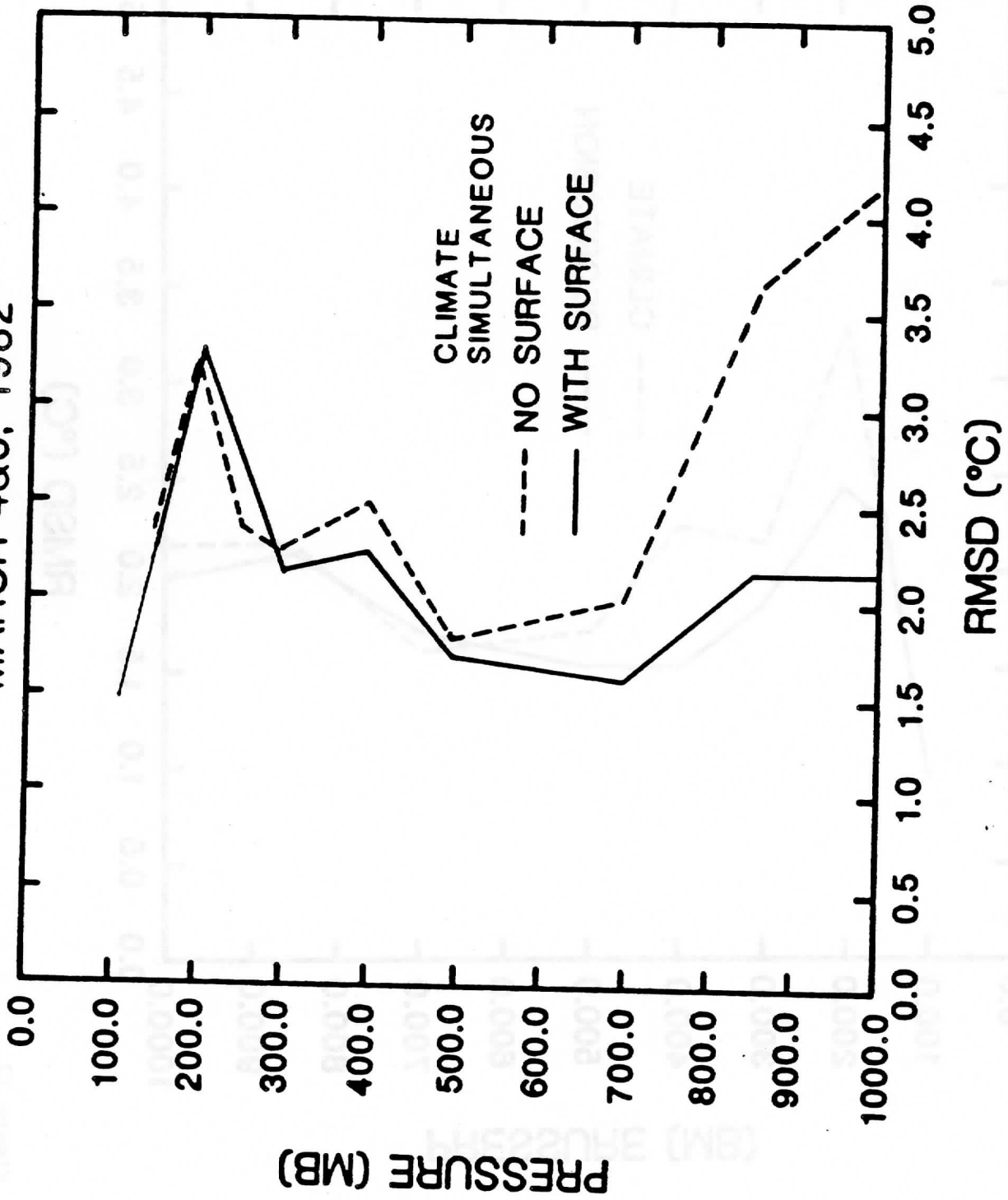


Figure 13

85.09. I1

THE SCHWERDTFEGER LIBRARY
1225 W. Dayton Street
Madison, WI 53706

**The Technical Proceedings of
The Second International TOVS Study Conference**

Igls, Austria

February 18 - 22, 1985

Edited by

W. P. Menzel

**Cooperative Institute for Meteorological Satellite Studies
Space Science and Engineering Center
University of Wisconsin
1225 West Dayton Street
Madison, Wisconsin 53706
(608) 262-0544**

September 1985